AWARD NUMBER: W81XWH-15-2-0006

TITLE: Mechanisms of Resistance to Chemotherapies Targeting BRCA-Mutant Breast Cancer

PRINCIPAL INVESTIGATOR: Dr. Andre Nussenzweig

CONTRACTING ORGANIZATION: The Geneva Foundation
Tacoma, WA 98402

REPORT DATE: December 2015

TYPE OF REPORT: Annual Report

PREPARED FOR: U.S. Army Medical Research and Materiel Command

Fort Detrick, Maryland 21702-5012

DISTRIBUTION STATEMENT: Approved for Public Release;

Distribution Unlimited

The views, opinions and/or findings contained in this report are those of the author(s) and should not be construed as an official Department of the Army position, policy or decision unless so designated by other documentation.

REPORT DOCUMENTATION PAGE

Form Approved
OMB No. 0704-0188

1. REPORT DATE *(DD-MM-YYYY)* DECEMBER 2015	2. REPORT TYPE ANNUAL REPORT	3. DATES COVERED *(From - To)* 1 Dec 2014 - 30 Nov 2015

4. TITLE AND SUBTITLE Mechanisms of Resistance to Chemotherapies Targeting BRCA-Mutant Breast Cancer	5a. CONTRACT NUMBER
	5b. GRANT NUMBER W81XWH-15-2-0006
	5c. PROGRAM ELEMENT NUMBER
6. AUTHOR(S) Andre Nussenzweig, Ph.D.	5d. PROJECT NUMBER
	5e. TASK NUMBER
	5f. WORK UNIT NUMBER

7. PERFORMING ORGANIZATION NAME(S) AND ADDRESS(ES) The Geneva Foundation 917 Pacific Ave, Suite 600 Tacoma, WA 98402	8. PERFORMING ORGANIZATION REPORT NUMBER

9. SPONSORING / MONITORING AGENCY NAME(S) AND ADDRESS(ES) Jamie Shortall USAMRAA 1077 Patchel Street Ft. Detrick, MD 21702 PH 301-619-2393	10. SPONSOR/MONITOR'S ACRONYM(S) USAMRAA
	11. SPONSOR/MONITOR'S REPORT NUMBER(S)

12. DISTRIBUTION / AVAILABILITY STATEMENT
Approved for public release; distribution unlimited

13. SUPPLEMENTARY NOTES

14. ABSTRACT

This research proposal for the BRCP Idea Expansion Award involves a detailed study of the underlying mechanisms of drug resistance in BRCA1 and BRCA2 deficient cells through the genetic manipulation of the major players that mediate homologous recombination and non-homologous end joining DNA repair pathways. These studies will serve as a foundational data set in determining the importance of DNA repair pathways in acquiring resistance to breast and ovarian cancer chemotherapies. Because drug resistance is an inescapable feature of all cancer treatments, an understanding of the causal mechanisms of resistance will undoubtedly provide new opportunities and susceptible targets in cancer therapies.

15. SUBJECT TERMS

16. SECURITY CLASSIFICATION OF:			17. LIMITATION OF ABSTRACT	18. NUMBER OF PAGES	19a. NAME OF RESPONSIBLE PERSON
a. REPORT	b. ABSTRACT	c. THIS PAGE	UU	27	19b. TELEPHONE NUMBER *(include area code)*

Standard Form 298 (Rev. 8-98)
Prescribed by ANSI Std. Z39.18

1. **INTRODUCTION:** Narrative that briefly (one paragraph) describes the subject, purpose and scope of the research.

In ongoing work being performed in support of the BCRP Idea Expansion Award, we have hypothesized that restoration of homologous recombination (HR) is a critical driver of chemo-resistance in BRCA1/2 mutated breast cancers. Earlier work provided evidence for a novel mechanism for HR restoration, through the inactivation of proteins functioning in an alternate DNA repair pathway called non-homologous end joining (NHEJ). Loss of NHEJ proteins restored normal HR activity in BRCA1 deficient cells and rendered these cells resistant to PARPi. The major aim of this research is to understand how altering the balance between NHEJ and HR pathways can be exploited to overcome the Achilles heel of acquired resistance in breast cancer treatment.

2. **KEYWORDS:** Provide a brief list of keywords (limit to 20 words).

1. 53BP1: p53 Binding Protein 1
2. Brca1: Breast cancer type 1 susceptibility protein, tumor suppressor
3. Brca2: Breast cancer type 2 susceptibility protein, tumor suppressor
4. BRCT domain: BRCA1 Carboxy Terminal Domain
5. CD19: Cluster of Differentiation 19
6. CRE: Causes Recombination
7. DSB: Double Strand Breaks
8. H2AX- a variant of Histone 2A, a core chromatin protein HR: Homologous Recombination
9. MEFs: Mouse Embryonic Fibroblasts
10. NHEJ: Non-Homologous End Joining
11. PA1: PTIP-Associated protein 1
12. PARP: Poly ADP-Ribose Polymerase
13. PARPi: Poly ADP-Ribose Polymerase Inhibitor
14. PTIP: Pax Transactivation Domain-Interacting Protein
15. RAP80: Receptor-Associated Protein 80
16. RIF1: RAP1 Interacting Factor 1
17. RNF8: Ring Finger protein 8
18. RNF168: Ring Finger protein 168
19. RPA: Replication Protein A
20. TCGA: The Cancer Genome Atlas

3. **ACCOMPLISHMENTS:** The PI is reminded that the recipient organization is required to obtain prior written approval from the USAMRAA Grants Officer whenever there are significant changes in the project or its direction.

- What were the major goals and objectives of the project?
- What was accomplished under these goals?
- What opportunities for training and professional development did the project provide?
- How were the results disseminated to communities of interest?
- What do you plan to do during the next reporting period to accomplish the goals and objectives?

What were the major goals of the project?

In this proposal, we outlined two major Specific Aims and Goals.

Overall, in **Specific Aim 1**, we proposed the use of a genetic approach to define interactions between NHEJ and HR effectors that regulate DNA repair pathway selection (24 months). In specific **Sub-Aim 1a**, we intend to test the hypothesis that elevated levels of chromatin bound 53BP1 converts wild type cells to a 'BRCA-deficient' state in the context of drug sensitivity and genome stability. In specific **Sub-Aim 1b**, the importance of PTIP associated proteins (PA1 and MLL4) and the functional domains within PTIP necessary for HR reconstitution are to be evaluated by *in vivo* experimentation.

Overall, in **Specific Aim 2**, we proposed testing the contribution of the 53BP1 associated protein (PTIP) in influencing repair pathway selection and to also computationally interrogate clinical data sets together with data

acquired from murine models to understand the mechanisms of chemo-resistance in BRCA1- and BRCA2-mutated cancers (24 months). In specific **Sub-Aim 2a**, we are testing the hypothesis that PTIP can influence repair pathway selection and drug sensitivity. In specific **Sub-Aim 2b**, we plan on using gene expression data and other genome-wide data sets from clinical databases to implicate known (and novel) proteins involved in the regulation of chemoresistance.

What was accomplished under these goals?

In order to address how interactions between NHEJ and HR proteins influenced repair pathway selection (**Specific Aim 1**), we asked whether increased expression of RNF168, a RING domain E3-ubiquitin ligase or 53BP1 impacts physiological NHEJ, such as immunoglobulin class switch recombination (CSR), versus mutagenic NHEJ (defined as NHEJ conducted during S phase which typically results in genome instability). Predicated on the observation that supra-physiological levels of the E3 ubiquitin ligase RNF168 results in the hyper-accumulation of 53BP1/BRCA1 which accelerates DSB repair, we asked whether increased expression of RNF168 or 53BP1 impacts physiological versus mutagenic NHEJ. We found that the anti-resection activities of 53BP1 are rate-limiting for mutagenic NHEJ but not for physiological CSR. An implication of our results is that deregulation of the RNF168/53BP1 pathway could alter the chemosensitivity of BRCA1 deficient tumors.

The work leading to the conclusions detailed above was published in May 2015: *Ectopic expression of RNF168 and 53BP1 increases mutagenic but not physiological non-homologous end joining*.
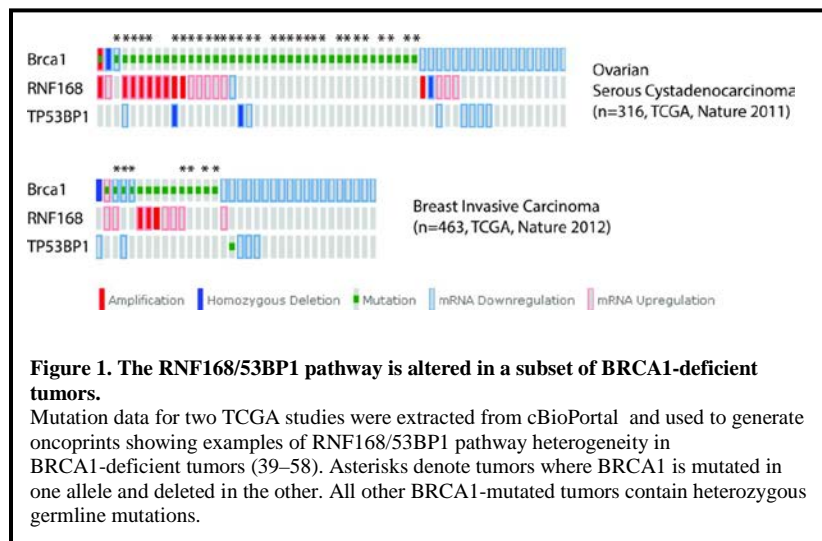Zong D, Callén E, Pegoraro G, Lukas C, Lukas J, Nussenzweig A.
<u>Nucleic Acids Res</u>. 2015 May 26;43(10):4950-61. doi: 10.1093/nar/gkv336.

The **Significant Results and Key Outcomes** summarized below highlight data germane to **Specific Aim 1** outlined in this proposal.

A1. RNF168 and 53BP1 levels modulate PARP inhibitor-induced genome instability in BRCA1 deficient cells

53BP1 has been shown to promote mutagenic NHEJ in BRCA1-deficient cells by blocking end resection, which leads to PARPi hypersensitivity and tumorigenesis. For both 53BP1 and its immediate upstream regulator RNF168 we found copy number variations, genetic mutations and/or heterogeneous mRNA expression changes in a subset of BRCA1-deficient ovarian and breast tumors within the TCGA database (**Figure 1**). We, therefore, sought to determine whether modulating the chromatin loading of RNF168 and/or 53BP1 would alter PARPi sensitivity. To this end, we established mouse embryonic

Figure 1. The RNF168/53BP1 pathway is altered in a subset of BRCA1-deficient tumors.
Mutation data for two TCGA studies were extracted from cBioPortal and used to generate oncoprints showing examples of RNF168/53BP1 pathway heterogeneity in BRCA1-deficient tumors (39–58). Asterisks denote tumors where BRCA1 is mutated in one allele and deleted in the other. All other BRCA1-mutated tumors contain heterozygous germline mutations.
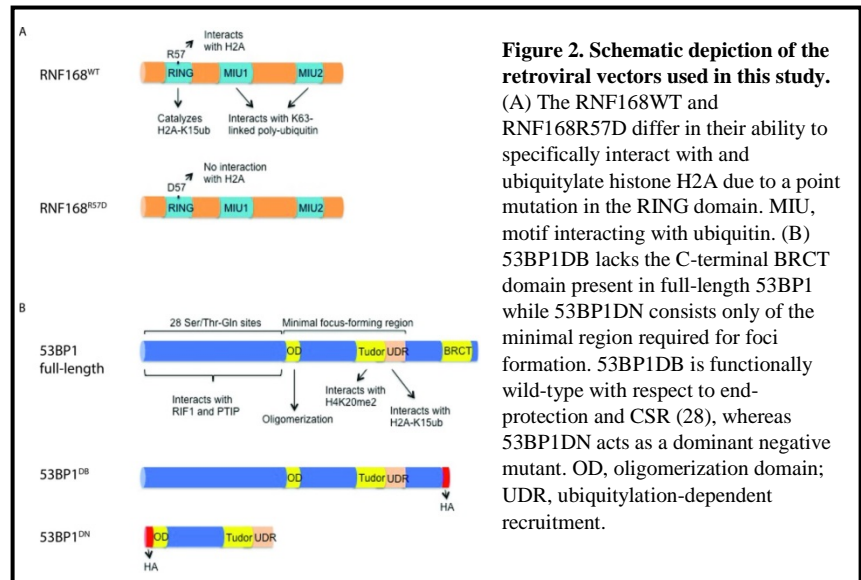
fibroblast (MEF) cell lines transduced with retroviral vectors encoding either wild-type RNF168 (RNF168WT) or a RNF168 mutant (RNF168R57D) that is incapable of 53BP1 recruitment (**Figure 2**). Since efficient transduction of MEFs with wild-type 53BP1 proved to be difficult due to its large size, we chose instead to overexpress 53BP1DB, a construct that lacks the extreme C-terminal BRCT domain but behaves like wild-type 53BP1 in terms of DSB end-protection, or a dominant negative fragment of 53BP1 (53BP1DN). We found that overexpression of RNF168WT in BRCA1Δ11/Δ11 MEFs promoted the formation of conjugated ubiquitin and 53BP1 as well as RIF1 foci upon DNA damage caused by PARP inhibition or ionizing radiation (**Figure 3A**). ***Thus, overexpression of 53BP1 itself can bypass the control of its spreading on damaged chromatin, which is normally limited by the availability of RNF168.***
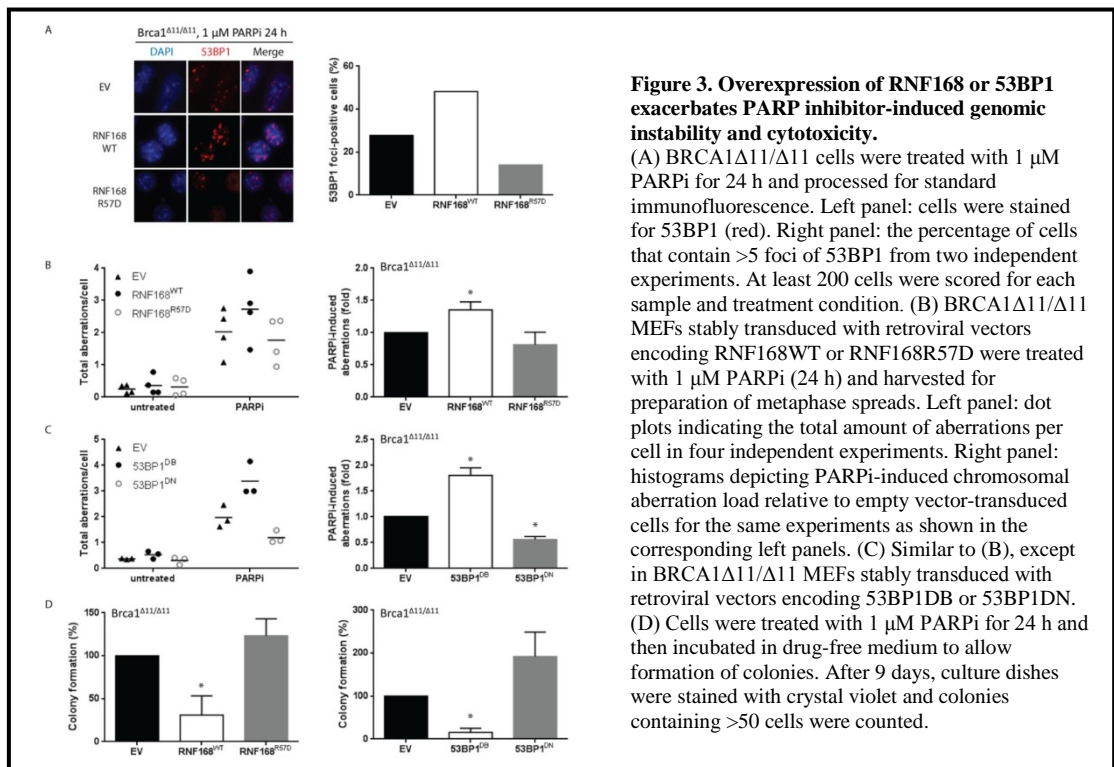
While PARPi treatment caused substantial genome instability in BRCA1Δ11/Δ11 control cells (MEFs infected with an empty vector), PARPi-induced genome instability was further increased by 1.5–2-fold following overexpression of RNF168WT or 53BP1DB (**Figure 3B and C**). Conversely, BRCA1Δ11/Δ11 MEFs overexpressing RNF168R57D or 53BP1DN had less PARPi-induced chromosomal aberrations than control cells, although in the case of RNF168R57D the difference did not reach statistical significance (**Figure 3B and C**). Consistent with these observations,
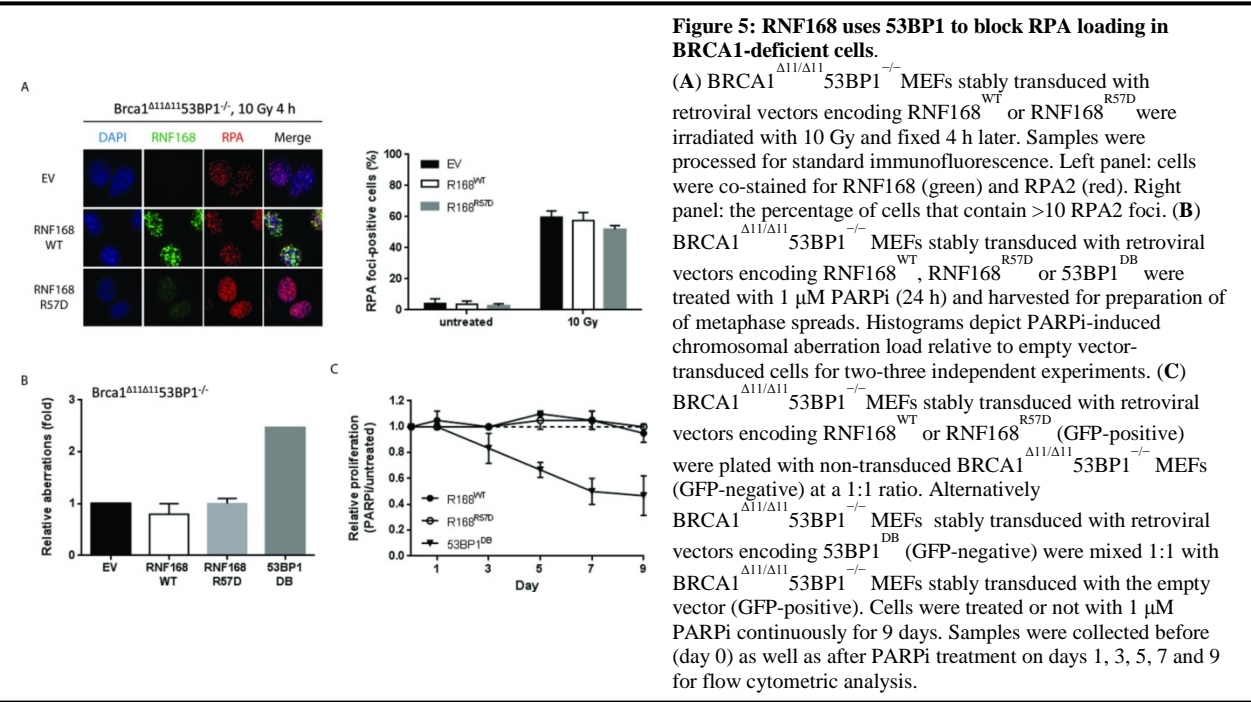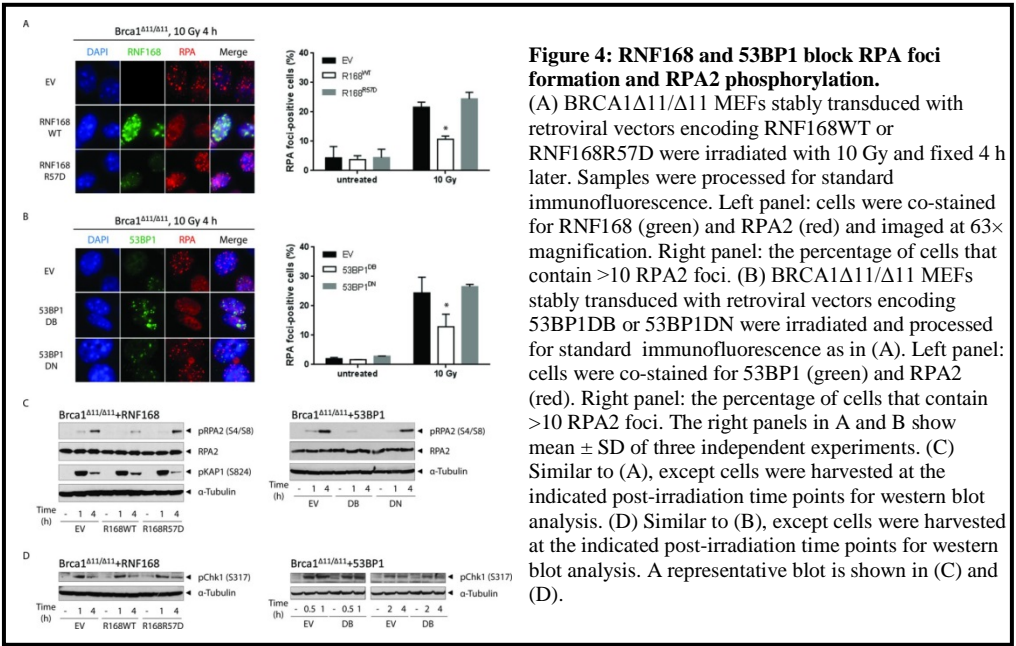

Figure 2. Schematic depiction of the retroviral vectors used in this study. (A) The RNF168WT and RNF168R57D differ in their ability to specifically interact with and ubiquitylate histone H2A due to a point mutation in the RING domain. MIU, motif interacting with ubiquitin. (B) 53BP1DB lacks the C-terminal BRCT domain present in full-length 53BP1 while 53BP1DN consists only of the minimal region required for foci formation. 53BP1DB is functionally wild-type with respect to end-protection and CSR (28), whereas 53BP1DN acts as a dominant negative mutant. OD, oligomerization domain; UDR, ubiquitylation-dependent recruitment.
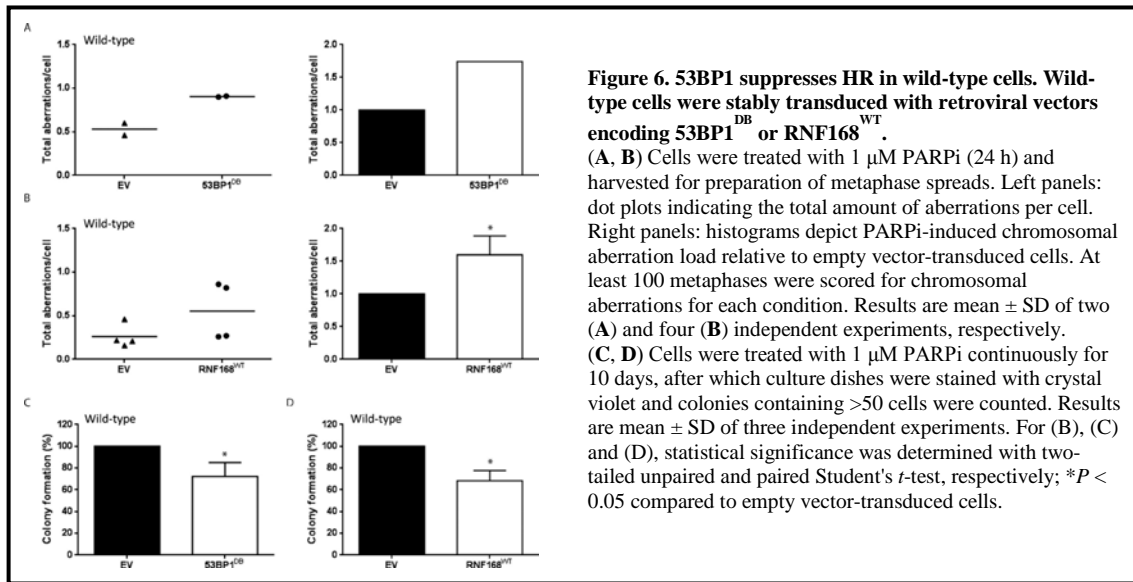
overexpression of RNF168WT or 53BP1DB conferred PARPi hypersensitivity in BRCA1Δ11/Δ11 MEFs in a colony formation assay whereas overexpression of RNF168R57D or 53BP1DN partially rescued long-term clonogenic survival (**Figure 3D**). *Taken together, these data show that the level of chromatin-bound RNF168 and 53BP1 dictates the extent of PARPi-induced genome instability and long-term survival in BRCA1-deficient cells.*

Therefore, in this published paper, we have proposed that excessive spreading of either endogenous 53BP1 brought on by increased RNF168-mediated H2A ubiquitylation or its exogenously overexpressed counterpart 53BP1DB, impedes HR.

Figure 3. Overexpression of RNF168 or 53BP1 exacerbates PARP inhibitor-induced genomic instability and cytotoxicity.
(A) BRCA1Δ11/Δ11 cells were treated with 1 μM PARPi for 24 h and processed for standard immunofluorescence. Left panel: cells were stained for 53BP1 (red). Right panel: the percentage of cells that contain >5 foci of 53BP1 from two independent experiments. At least 200 cells were scored for each sample and treatment condition. (B) BRCA1Δ11/Δ11 MEFs stably transduced with retroviral vectors encoding RNF168WT or RNF168R57D were treated with 1 μM PARPi (24 h) and harvested for preparation of metaphase spreads. Left panel: dot plots indicating the total amount of aberrations per cell in four independent experiments. Right panel: histograms depicting PARPi-induced chromosomal aberration load relative to empty vector-transduced cells for the same experiments as shown in the corresponding left panels. (C) Similar to (B), except in BRCA1Δ11/Δ11 MEFs stably transduced with retroviral vectors encoding 53BP1DB or 53BP1DN. (D) Cells were treated with 1 μM PARPi for 24 h and then incubated in drug-free medium to allow formation of colonies. After 9 days, culture dishes were stained with crystal violet and colonies containing >50 cells were counted.

A2. RNF168 and 53BP1 antagonize long-range end resection and RPA phosphorylation in BRCA1-deficient cells

BRCA1-mediated removal of 53BP1 is thought to be an essential prerequisite for end resection and RAD51-dependent HR. In agreement with this, we observed that 53BP1DB suppressed RAD51 foci formation in BRCA1Δ11/Δ11 MEFs. End resection enables RPA to form foci along progressively longer stretches of single-stranded DNA (ssDNA) before it is actively

Figure 4: RNF168 and 53BP1 block RPA foci formation and RPA2 phosphorylation.
(A) BRCA1Δ11/Δ11 MEFs stably transduced with retroviral vectors encoding RNF168WT or RNF168R57D were irradiated with 10 Gy and fixed 4 h later. Samples were processed for standard immunofluorescence. Left panel: cells were co-stained for RNF168 (green) and RPA2 (red) and imaged at 63× magnification. Right panel: the percentage of cells that contain >10 RPA2 foci. (B) BRCA1Δ11/Δ11 MEFs stably transduced with retroviral vectors encoding 53BP1DB or 53BP1DN were irradiated and processed for standard immunofluorescence as in (A). Left panel: cells were co-stained for 53BP1 (green) and RPA2 (red). Right panel: the percentage of cells that contain >10 RPA2 foci. The right panels in A and B show mean ± SD of three independent experiments. (C) Similar to (A), except cells were harvested at the indicated post-irradiation time points for western blot analysis. (D) Similar to (B), except cells were harvested at the indicated post-irradiation time points for western blot analysis. A representative blot is shown in (C) and (D).

displaced by RAD51. Notably, overexpression of either RNF168WT or 53BP1DB in irradiated BRCA1Δ11/Δ11 MEFs further suppressed the chromatin loading of RPA compared to control cells (**Figure 4A, B**). Importantly, we also noted that the cycling of BRCA1Δ11/Δ11 MEFs was not affected by overexpression of RNF168 or 53BP1, thus ruling out the possibility that differences in cell cycle progression contributed to the observed differences in RPA foci formation. DNA-PK-dependent RPA2 (S4, S8) phosphorylation was also significantly attenuated in BRCA1Δ11/Δ11 MEFs overexpressing RNF168WT or 53BP1DB (**Figure 4C**). In contrast the phosphorylation of KAP-1, an ATM substrate that responds to DSBs, remained unchanged (**Figure 4C**). Interestingly, ATR-mediated phosphorylation of CHK1 was not perturbed by RNF168WT or 53BP1DB overexpression (**Figure 4D**). Since

Figure 5: RNF168 uses 53BP1 to block RPA loading in BRCA1-deficient cells.
(A) BRCA1$^{\Delta11/\Delta11}$53BP1$^{-/-}$ MEFs stably transduced with retroviral vectors encoding RNF168^{WT} or RNF168^{R57D} were irradiated with 10 Gy and fixed 4 h later. Samples were processed for standard immunofluorescence. Left panel: cells were co-stained for RNF168 (green) and RPA2 (red). Right panel: the percentage of cells that contain >10 RPA2 foci. (B) BRCA1$^{\Delta11/\Delta11}$53BP1$^{-/-}$ MEFs stably transduced with retroviral vectors encoding RNF168^{WT}, RNF168^{R57D} or 53BP1^{DB} were treated with 1 μM PARPi (24 h) and harvested for preparation of of metaphase spreads. Histograms depict PARPi-induced chromosomal aberration load relative to empty vector-transduced cells for two-three independent experiments. (C) BRCA1$^{\Delta11/\Delta11}$53BP1$^{-/-}$ MEFs stably transduced with retroviral vectors encoding RNF168^{WT} or RNF168^{R57D} (GFP-positive) were plated with non-transduced BRCA1$^{\Delta11/\Delta11}$53BP1$^{-/-}$ MEFs (GFP-negative) at a 1:1 ratio. Alternatively BRCA1$^{\Delta11/\Delta11}$53BP1$^{-/-}$ MEFs stably transduced with retroviral vectors encoding 53BP1^{DB} (GFP-negative) were mixed 1:1 with BRCA1$^{\Delta11/\Delta11}$53BP1$^{-/-}$ MEFs stably transduced with the empty vector (GFP-positive). Cells were treated or not with 1 μM PARPi continuously for 9 days. Samples were collected before (day 0) as well as after PARPi treatment on days 1, 3, 5, 7 and 9 for flow cytometric analysis.

Figure 6. 53BP1 suppresses HR in wild-type cells. Wild-type cells were stably transduced with retroviral vectors encoding 53BP1^{DB} or RNF168^{WT}.
(**A**, **B**) Cells were treated with 1 μM PARPi (24 h) and harvested for preparation of metaphase spreads. Left panels: dot plots indicating the total amount of aberrations per cell. Right panels: histograms depict PARPi-induced chromosomal aberration load relative to empty vector-transduced cells. At least 100 metaphases were scored for chromosomal aberrations for each condition. Results are mean ± SD of two (**A**) and four (**B**) independent experiments, respectively. (**C**, **D**) Cells were treated with 1 μM PARPi continuously for 10 days, after which culture dishes were stained with crystal violet and colonies containing >50 cells were counted. Results are mean ± SD of three independent experiments. For (**B**), (**C**) and (**D**), statistical significance was determined with two-tailed unpaired and paired Student's *t*-test, respectively; *$P < 0.05$ compared to empty vector-transduced cells.

CHK1 activation by ATR requires only minimal resection, these results suggest that RNF168 regulates 53BP1 chromatin binding to antagonize long-range DSB end resection in BRCA1-deficient cells. Consistent with this notion, RNF168WT failed to block RPA loading (**Figure 5A**) or to enhance PARPi sensitivity in BRCA1Δ11/Δ11 MEFs when 53BP1 was co-deleted (**Figure 5B and C**). By contrast, 53BP1DB overexpression re-imparted susceptibility to PARPi-induced genome instability and decreased the survival of BRCA1Δ11/Δ1153BP1−/− MEFs (**Figure 5B and C**).

In wild-type and 53BP1−/− MEFs, where BRCA1 is fully operational, ectopic expression of 53BP1DB also led to increased genome instability in response to PARPi treatment (**Figure 6A**). Moreover, we observed that 53BP1DB suppressed RAD51 loading in wild-type MEFs, as evidenced by the reduced numbers and smaller sizes of RAD51 foci, although this effect was milder than in BRCA1-deficient MEFs. As a result, 53BP1DB overexpression partially enhanced the toxicity of PARPi in wild-type MEFs (**Figure 6A and C**). Similarly, overexpression of RNF168WT increased PARPi-induced genome instability and cytotoxicity in wild-type MEFs (**Figure 6B and D**). *Taken together, our data suggest that while a functional BRCA1 pathway can fully counteract endogenous RNF168/53BP1 during a normal S-phase DNA damage response, increased levels of RNF168 and 53BP1 can still suppress HR, increase toxicity and limit long-range end resection in BRCA1-proficient cells.*

A3. RNF168 and 53BP1 are not limiting factors during immunoglobulin class switch recombination

53BP1 promotes productive long-range NHEJ during CSR and VDJ recombination at least in part by blocking end resection. A recent study found that increased 53BP1 spreading caused by stabilization of RNF168 accelerates NHEJ; we therefore asked whether overexpression of exogenous RNF168 and/or 53BP1 might augment CSR. However, we observed that overexpression of RNF168 or 53BP1 did not affect CSR in wild-type B cells. We also tested whether exogenous RNF168 and/or 53BP1 might augment CSR in the context of a resection defect imparted by BRCA1 deficiency. Retroviral-mediated overexpression of RNF168WT led to enhanced chromatin loading of 53BP1 (**Figure 7A**). Despite this, however, overexpression of RNF168WT or 53BP1DB did not significantly enhance CSR in BRCA1-deficient B cells (**Figure 7B and C**). Conversely, CSR was not reduced by enforced expression of RNF168R57D (**Figure 7B and C**). *Together, these data demonstrate that levels of chromatin-bound 53BP1 are not rate-limiting for physiological NHEJ during CSR* (**Figure 7D**).

Overall Summary: Ectopic expression of RNF168 and 53BP1 increases mutagenic but not physiological non-homologous end joining

We found that the requirements of 53BP1 in mutagenic repair of PARPi-induced DNA damage and physiological NHEJ during CSR are dissimilar (**Figure 7D**). As it has been proposed that the anti-resection function of 53BP1 is critical for CSR, we reasoned that further inhibiting end resection with exogenously overexpressed 53BP1 might
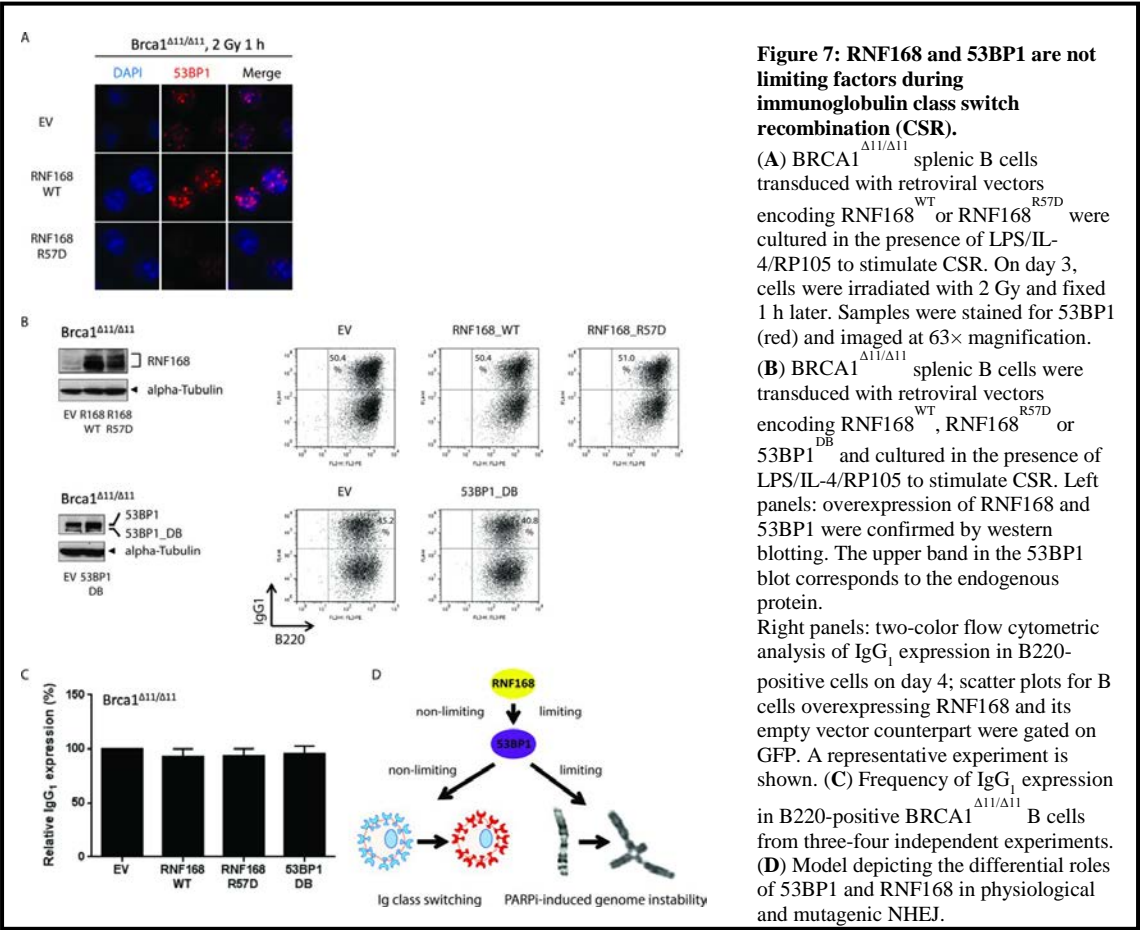
lead to enhanced CSR. To our surprise, however, neither RNF168 nor 53BP1 had any significant impact on CSR efficiency when overexpressed. Therefore, the expression levels of RNF168 or 53BP1 proteins are clearly more

Figure 7: RNF168 and 53BP1 are not limiting factors during immunoglobulin class switch recombination (CSR).
(**A**) BRCA1$^{\Delta 11/\Delta 11}$ splenic B cells transduced with retroviral vectors encoding RNF168^{WT} or RNF168^{R57D} were cultured in the presence of LPS/IL-4/RP105 to stimulate CSR. On day 3, cells were irradiated with 2 Gy and fixed 1 h later. Samples were stained for 53BP1 (red) and imaged at 63× magnification.
(**B**) BRCA1$^{\Delta 11/\Delta 11}$ splenic B cells were transduced with retroviral vectors encoding RNF168^{WT}, RNF168^{R57D} or 53BP1^{DB} and cultured in the presence of LPS/IL-4/RP105 to stimulate CSR. Left panels: overexpression of RNF168 and 53BP1 were confirmed by western blotting. The upper band in the 53BP1 blot corresponds to the endogenous protein.
Right panels: two-color flow cytometric analysis of IgG$_1$ expression in B220-positive cells on day 4; scatter plots for B cells overexpressing RNF168 and its empty vector counterpart were gated on GFP. A representative experiment is shown. (**C**) Frequency of IgG$_1$ expression in B220-positive BRCA1$^{\Delta 11/\Delta 11}$ B cells from three-four independent experiments. (**D**) Model depicting the differential roles of 53BP1 and RNF168 in physiological and mutagenic NHEJ.

than sufficient to handle all AID-generated breaks under physiological conditions. Since the levels of RNF168 render ubiquitin signaling rate-limiting when the number of DSBs exceeds 20–40, one possible explanation for these findings is that PARPi-induced DSBs in BRCA1-deficient cells may far exceed the number of DSBs generated by AID during CSR. The increased DSBs in PARPi-treated cells, in contrast to the fewer number of CSR-associated breaks could saturate histone ubiquitylation. To date, the only known limiting factor for CSR is AID itself, which when overexpressed causes supra-physiological accumulation of cleavage events at Ig switch regions, additional substrates for 53BP1-dependent NHEJ and increased CSR. Taken together, these data showed that the anti-resection activity of 53BP1 is limiting during mutagenic but not physiological NHEJ.

The **Significant Results and Key Outcomes** summarized below highlight data germane to **Specific Aim 2** outlined in this proposal.

B1. Replication fork protection by the prevention of nascent DNA strand degradation is strongly co-related with chemoresistance in BRCA1/2-deficient cells

It is known that BRCA1/2-deficient cells have a significantly reduced capacity to repair DNA breaks (DSBs) and are hypersensitive to DNA damaging agents such as platinum salts and poly(ADP-ribose) polymerase (PARP) inhibitors. While these agents are clinically effective, the majority of BRCA1/2-mutant carcinomas acquire resistance to
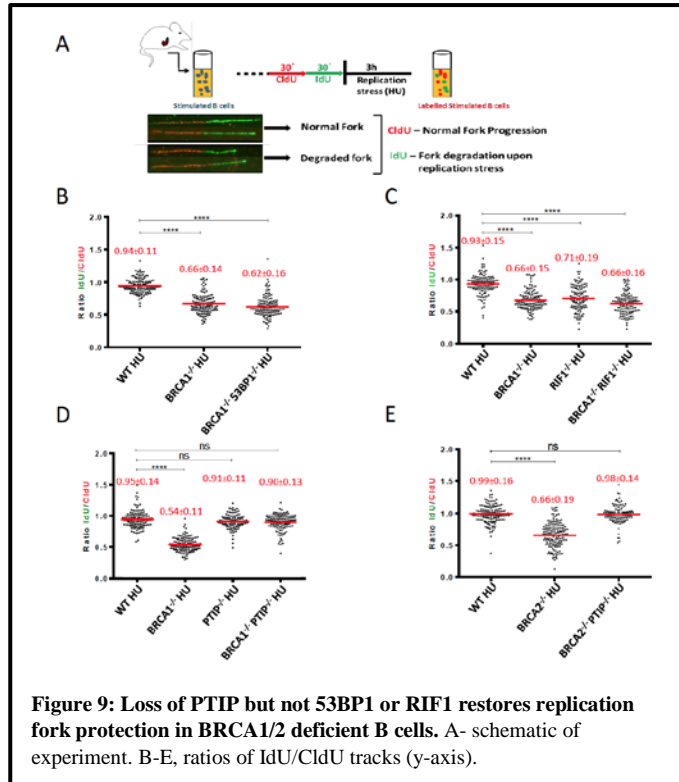

Figure 8: **Loss of PTIP in BRCA1/2 deficient cells reduces genomic instability in response to PARP1 and cisplatin (A, B)**

these drugs. Besides reduced uptake of drugs, the only described mechanism that drives chemotherapeutic resistance in BRCA1/2-deficient tumors is through the restoration of homologous recombination (HR). Preliminary work related to the Aims outlined in this proposal, show that loss of the MLL3/4 complex protein PTIP protects BRCA1/2-deficient cells from DNA damaging agents. ***However, PTIP deficiency remarkably does not restore HR activity in BRCA2- deficient cells suggesting that chemoresistance and genomic stability can be re-established independent of a functional HR pathway. Current studies suggest that replication fork protection by the prevention of nascent DNA strands from degradation is strongly co-related with the observed drug resistance***.

We and others had previously shown that PTIP acts downstream of 53BP1 in promoting PARPi toxicity in BRCA1-deficient cells. We, therefore, examined the sensitivity of BRCA1/PTIP-deficient cells to PARPi and cisplatin. Unexpectedly, while BRCA1/53BP1-deficient cells are sensitive to cisplatin, BRCA1/PTIP-mutant cells are remarkably resistant to both PARPi and cisplatin as evidenced by reduction in chromosomal aberrations (**Figure 8**). While BRCA1 functions early during DSB resection, BRCA2 functions later in HR by catalyzing RAD51 nucleo-filaments at processed DSBs. We have generated BRCA2/PTIP-doubly deficient B cells (CD19 CRE BRCA2f/fPTIPf/f) and measured PARPi and cisplatin induced chromosomal instability (**Figure 8**). Strikingly, in contrast to BRCA2/53BP1 mutants, which are hypersensitive to both DNA damaging agents, BRCA2/PTIP-deficient cells show resistance to both PARPi and cisplatin (**Figure 8**). Interestingly, drug resistance in BRCA2/PTIP-deficient cells cannot be attributed

Figure 9: Loss of PTIP but not 53BP1 or RIF1 restores replication fork protection in BRCA1/2 deficient B cells. A- schematic of experiment. B-E, ratios of IdU/CldU tracks (y-axis).

to restoration of RAD51 function or reactivation of HR, as BRCA2/PTIP deficient cells failed to form IR induced RAD51 foci (not shown). ***Thus, defective HR is maintained in the BRCA2/PTIP double mutant cells***.

The finding that loss of PTIP partially restores PARPi and cisplatin resistance in BRCA1/2-deficient cells but does not rescue DSB-induced RAD51 foci formation suggests that PTIP may modulate DSB repair-independent function of BRCA1/2. Recently, it was shown that BRCA1 and BRCA2 protect stalled replication forks (RF) from Mre11-mediated degradation independent of their roles in HR. We therefore hypothesized that PTIP might modulate RF degradation. To directly test this, we monitored the stability of nascent replication tracks in cells defective in BRCA1/2. B cells were sequentially labeled with CldU (red) followed by IdU-(green) labeling for 30 minutes each, following which the actively RFs were stalled with HU (**schema in Figure 9A**). The relative shortening of the 2nd IdU track after HU treatment serves as a measure of RF degradation (**Figure 9A**). WT cells showed a mean IdU/CldU fiber length ratio close to 1. However, BRCA1- and BRCA2-deficient B cells failed to maintain the integrity of nascent DNA tracks during replication stalling with HU (**Figure 9B-E**).

Summary of Methodology Employed

Cell cultures, retroviral infection and flow cytometry
Resting B cells were isolated from spleen using anti-CD43 microbeads and stimulated to proliferate with 25 μg/ml LPS, 5 ng/ml IL-4 and 0.5 μg/ml RP105. To overexpress RNF168, constructs encoding human RNF168WT or RNF168R57D were subcloned into the pMX-PIE-IRES-GFP retroviral vector and used to transfect BOSC23 cells along with the pCL-Eco helper virus. Retroviral supernatant was collected 40–48 h later for infection of MEFs and B cells. Class switch recombination was assayed on days 3 and 4 using biotinylated anti-IgG1 and fluorochrome-conjugated anti-B220 antibodies.

FISH analysis
Stimulated B cells and MEFs were arrested at mitosis with colcemid treatment and harvested for metaphase spreads. Images were captured with an automated fluorescence microscope. One hundred metaphases were scored for the presence of chromosomal aberrations.

Cell cycle analysis
Cells were fixed in 70% ethanol and stained with propidium iodide for flow cytometric analysis. ModFit LT was used to assign cell cycle distribution.

Colony formation and growth competition assays
MEFs were treated with 1 μM PARPi (KU-0058948) either continuously for 10 days (wild-type, 53BP1−/−) or for 24 h followed by a 9-day post-incubation in drug-free medium (BRCA1Δ11/Δ11). Thereafter, culture dishes were stained with 0.5% crystal violet and colonies containing >50 cells were counted. Due to poor colony forming ability of BRCA1Δ11/Δ1153BP1−/− MEFs, a growth competition assay was used instead. To this end, BRCA1Δ11/Δ1153BP1−/− MEFs stably transduced with retroviral vectors encoding RNF168WT or RNF168R57D (GFP-positive) were mixed with non-transduced BRCA1Δ11/Δ1153BP1−/− MEFs (GFP-negative) at a 1:1 ratio. Alternatively BRCA1Δ11/Δ1153BP1−/− MEFs stably transduced with retroviral vectors encoding 53BP1DB (GFP-negative) were mixed with BRCA1Δ11/Δ1153BP1−/− MEFs stably transduced with the empty vector (GFP-positive). Cells were treated or not with 1 μM PARPi continuously for 9 days. Samples were collected before (day 0) as well as after PARPi treatment on days 1, 3, 5, 7 and 9 for flow cytometric analysis. Relative proliferation was calculated by normalizing the fraction of GFP-positive cells in PARPi-treated versus untreated samples collected on the same day.

Immunofluorescence
For standard immunofluorescence studies, MEFs grown on coverslips were subjected to γ-irradiation (cesium-137) or treated with PARPi. At the indicated times post-treatment, cells were first pre-extracted (20 mM HEPES, pH 7.0, 50 mM NaCl, 3 mM MgCl2, 0.3 M sucrose, 0.2% Triton X-100) for 5 min on ice to remove nucleoplasmic proteins and then sequentially fixed (4% paraformaldehyde), permeabilized (0.5% Triton X-100) and blocked (2% BSA). Samples were incubated with primary antibodies recognizing HA-tag, RNF168, conjugated ubiquitin (FK2), 53BP1, RIF1, RPA2, RAD51 followed by appropriate fluorochrome-conjugated secondary antibodies. DNA was counterstained with DAPI. Foci images were captured with a fluorescence microscope at 63× magnification, unless otherwise stated. High-throughput automated imaging was used to captured chromatin-bound RPA at 20× magnification.

Immunoblotting
Whole cell extract (WCE) was resolved by SDS-PAGE and transferred onto nitrocellulose membranes. Samples were incubated with primary antibodies recognizing RNF168, 53BP1, phospho-RPA2 (S4, S8), phospho-CHK1 (S317), RPA2 and α-tubulin. Following incubation with the appropriate horseradish peroxidase-linked secondary antibodies, bands were visualized using enhanced chemiluminescence.

DNA fiber analysis
Asynchronous B-cells were labeled with 30 μM CldU, washed with PBS and exposed to 250 μM IdU. After exposure to IdU, the cells were washed again in warm PBS and treated or not with HU before collection. Cells were then lysed and DNA fibers stretched onto glass slides. The fibers were denatured with 2.5 M HCl for 1 h, washed with PBS and blocked with 2% BSA in phosphate buffered saline Tween 20 for 30 min. The newly replicated CldU and IdU tracks were revealed with anti-BrdU antibodies recognizing CldU and IdU respectively. Images were taken at 60×magnification (Zeiss Axio Observer.Z1), and statistical analysis was carried out using GraphPad Prism.

What opportunities for training and professional development has the project provided?

The project has presented numerous opportunities for the Principal Investigator (**Dr. Andre Nussenzweig**) and two post-doctoral fellows (**Drs. Arnab Ray Chaudhuri and Dali Zong**) to present their work in symposia at the NIH and at national and international conferences (**see details in Section 6 below**).

How were the results disseminated to communities of interest?

Results were shared with the scientific community via informal discussions, posters and presentations at scientific meetings and through publications in peer-reviewed journals

What do you plan to do during the next reporting period to accomplish the goals?

We will continue to pursue the goals outlined in Specific Aims 1 and 2, specifically focusing on dissecting the mechanisms underlying replication fork degradation/protection in BRCA1/2-deficient cells.

4. **IMPACT:** This component is used to describe ways in which the work, findings, and specific products of the project have had an impact during this reporting period. Describe distinctive contributions, major accomplishments, innovations, successes, or any change in practice or behavior that has come about as a result of the project relative to:

- the development of the principal discipline(s) of the project;
- other disciplines;
- technology transfer; or
- society beyond science and technology.

What was the impact on the development of the principal discipline(s) of the project?

Work in support of both Specific Aims of this proposal highlight mechanisms that can alter drug sensitivity or resistance in BRCA-deficient tumors. We have also observed that deregulation of the RNF168/53BP1 pathway can alter the chemosensitivity of BRCA1 deficient tumors (**Specific Aim 1**). We have also observed that PTIP-deficiencies promote synthetic viability and drug resistance in BRCA-deficient cells without restoring HR (**Specific Aim 2**).

What was the impact on other disciplines?

Nothing to Report

What was the impact on technology transfer?

Nothing to Report

What was the impact on society beyond science and technology?

Nothing to Report

5. **CHANGES/PROBLEMS:** The Project Director/Principal Investigator (PD/PI) is reminded that the recipient organization is required to obtain prior written approval from the awarding agency Grants Officer whenever there are significant changes in the project or its direction. If not previously reported in writing, provide the following additional information or state, "Nothing to Report," if applicable:

- Changes in approach and reasons for change.
- Actual or anticipated problems or delays and actions or plans to resolve them.
- Changes that have a significant impact on expenditures.
- Significant changes in use or care of human subjects, vertebrate animals, biohazards, and/or select agents.

Changes in approach and reasons for change

Nothing to Report

Actual or anticipated problems or delays and actions or plans to resolve them

Nothing to Report

Changes that had a significant impact on expenditures

Nothing to Report

Significant changes in use or care of human subjects, vertebrate animals, biohazards, and/or select agents

Nothing to Report

6. PRODUCTS: List any products resulting from the project during the reporting period. Examples of products include:

- publications, conference papers, and presentations;
- website(s) or other Internet site(s);
- technologies or techniques;
- inventions, patent applications, and/or licenses; and
- other products.

If there is nothing to report under a particular item, state "Nothing to Report."

- **Publications, conference papers, and presentations**

  Journal publications.

  1. *Ectopic expression of RNF168 and 53BP1 increases mutagenic but not physiological non-homologous end joining*.
  Zong D, Callén E, Pegoraro G, Lukas C, Lukas J, Nussenzweig A. *Nucleic Acids Res*. 2015 May 26;43(10):4950-61. doi: 10.1093/nar/gkv336.

  2. *Replication fork protection can bypass the requirement for homologous recombination. (2015) In 2nd revision* (*Nature*)
  A. Ray Chaudhuri*, E. Callen*, X. Ding, E. Gogola, A. Duarte, J. Lee, N.Wong, V. Lafarga, J. Calvo, N. Panzarino, S. John, A. Day, A. Crespo, H. Chen, B.Shen, J. A. Daniel, P.A. Konstantinopoulos, D.Cortez, S.B. Cantor, O.Fernandez-Capetillo, K. Ge, J. Jonkers, S. Rottenberg, S.K. Sharan and A. Nussenzweig.

  Books or other non-periodical, one-time publications.

  Nothing to Report

  Other publications, conference papers, and presentations.

  The project has presented numerous opportunities for the Principal Investigator (**Dr. Andre Nussenzweig**) and two post-doctoral fellows (**Drs. Arnab Ray Chaudhuri and Dali Zong**) to present their work in symposia at the NIH and at national and international conferences.

  1. Arnab Ray Chuadhuri: Visiting post-doctoral fellow

  Invited Talks:

  a. National Center for Biological Sciences, Bangalore, India-October 2015
  b. Regional Center for Biotechnology, Gurgaon, India- September 2015
  c. Indian Statistical Institute, Kolkata, India- September 2015

d. Workshop on Chromosome Biology organized by Center of Excellence in Chromosome Biology, NIH-June 2014

Poster Presentations at Meetings:

a. Cold Spring Harbor Meeting for Eukaryotic DNA replication, New York, USA-September 2015
b. Keystone Symposia for Replication and Recombination, Whistler, Canada-March 2015

2. Dali Zong: Visiting post-doctoral fellow

Invited talks:

a. Workshop on Chromosome Biology organized by Center of Excellence in Chromosome Biology, NIH-November 2015

3. Andre Nussenzweig: Principal Investigator

Invited Talks:

a. Invited Speaker and Session Chair, Keystone Symposia- DNA Replication and Recombination, Whistler, BC, Canada, 2015
b. Invited Speaker, St. Jude Children's Cancer Center Seminar Series, Memphis, TN, 2015
c. Invited Speaker, St. Louis University School of Medicine-Department of Biochemistry and Molecular Biology Seminar Series, St. Louis, MO, 2015
d. Invited Speaker, New York University School of Medicine-Biochemistry and Molecular Pharmacology Seminar Series, New York, NY, 2015
e. Invited Speaker, UVA BMG Annual Symposium- Cell Cycle and Genomic Stability, Charlottesville, VA, 2015
f. Invited Speaker, 2015 FASEB Summer Research Conference. Big Sky, Montana, 2015
g. Invited Speaker, Conference "Chromatin and Cell Fate", Essen, Germany, 2015
h. Invited Speaker, Seminar Series- Cornell Univ. seminar at the College of Veterinary Medicine at Cornell University, Ithaca, NY, 2015
i. Invited Speaker, Banbury Meeting, Cold Spring Harbor, 2015
j. Invited Speaker, Weill Cornell University, New York, 2015

- **Website(s) or other Internet site(s)**

  Nothing to Report

- **Technologies or techniques**

  Nothing to Report

- **Inventions, patent applications, and/or licenses**

  Nothing to Report

- **Other Products**

  Nothing to Report

7. **PARTICIPANTS & OTHER COLLABORATING ORGANIZATIONS**

Provide the following information on participants:

- what individuals have worked on the project?

- has there been a change in the other active support of the PD/PI(s) or senior/key personnel since the last reporting period? what other organizations have been involved as partners?

What individuals have worked on the project?

Provide the following information for: (1) PDs/PIs; and (2) each person who has worked at least one person month per year on the project during the reporting period, regardless of the source of compensation (a person month equals approximately 160 hours of effort).

Name:	**Dr. Andre Nussenzweig**
Project Role:	Principal Investigator
Researcher Identifier (e.g. ORCID ID):	NA
Nearest person month worked:	3
Contribution to Project:	Responsible for the overall direction of the proposed research as well as daily supervision of laboratory activities, personnel, design and interpretation of experiments, preparation of manuscripts and presentations
Funding Support:	Salary supported by the Intramural Research Program (IRP)

Name:	**Dr. Arnab Ray Chaudhuri**
Project Role:	Visiting Fellow
Researcher Identifier (e.g. ORCID ID):	NA
Nearest person month worked:	12
Contribution to Project:	Developed the replication fiber assay that measures the rates of fork progression and the extent of fork protection/degradation. He has also helped with the design and execution of primary experiments and contributed to the writing of a manuscript (in revision in *Nature*) related to Specific Aim 2 in this proposal
Funding Support:	Salary renumeration from a fellowship with the Human Frontier Science Program

Name:	**Dr. Elsa Callen**
Project Role:	Visiting Fellow
Researcher Identifier (e.g. ORCID ID):	NA
Nearest person month worked:	3
Contribution to Project:	Responsible for genetic and biochemical assays designed to understand the contributing genetic factors in DNA repair pathway selection. Dr. Callen also helped with the design and execution of primary experiments related to replication fork protection. She also contributed to the writing of a manuscript (in revision in *Nature*) related to Specific Aim 2 in this proposal
Funding Support:	Salary supported by the Intramural Research Program (IRP)

Name:	**Dr. Dali Zong**
Project Role:	Visiting Fellow
Researcher Identifier (e.g. ORCID ID):	NA
Nearest person month worked:	12
Contribution to Project:	Responsible for genetic and biochemical assays designed to understand the contributing genetic factors in DNA repair pathway selection. He made extensive contributions to the published manuscript (in *Nucleic Acids Research*) related to Specific Aim 1 in this proposal

Funding Support: Supported by the Intramural Research Program (IRP)

Has there been a change in the active other support of the PD/PI(s) or senior/key personnel since the last reporting period?

      Name: **Dr. Robert Farybai**

      Project Role: Former Research Fellow who is no longer associated with this project and the laboratory of Dr. Nussenzweig. Dr. Faryabi has taken up an independent tenure-track position in the Department of Pathology at the University of Pennsylvania as of June 2015

What other organizations were involved as partners?

Nothing to Report

8. **SPECIAL REPORTING REQUIREMENTS:**

      Nothing to Report

9. **APPENDICES:** Attach all appendices that contain information that supplements, clarifies or supports the text. Examples include original copies of journal articles, reprints of manuscripts and abstracts, a curriculum vitae, patent applications, study questionnaires, and surveys, etc.

      (**see Pdf of published Nucleic Acids Research paper**)

Ectopic expression of RNF168 and 53BP1 increases mutagenic but not physiological non-homologous end joining

Dali Zong[1], Elsa Callén[1], Gianluca Pegoraro[2], Claudia Lukas[3], Jiri Lukas[3] and André Nussenzweig[1,*]

[1]Laboratory of Genome Integrity; National Cancer Institute; National Institutes of Health; Bethesda, MD 20892, USA,
[2]Center for Cancer Research, National Cancer Institute; National Institute of Health, Bethesda, MD 20892, USA and
[3]The Novo Nordisk Foundation Center for Protein Research, University of Copenhagen, Faculty of Health and Medical Sciences, Blegdamsvej 3, 2200, Copenhagen, Denmark

ABSTRACT

DNA double strand breaks (DSBs) formed during S phase are preferentially repaired by homologous recombination (HR), whereas G_1 DSBs, such as those occurring during immunoglobulin class switch recombination (CSR), are repaired by non-homologous end joining (NHEJ). The DNA damage response proteins 53BP1 and BRCA1 regulate the balance between NHEJ and HR. 53BP1 promotes CSR in part by mediating synapsis of distal DNA ends, and in addition, inhibits 5' end resection. BRCA1 antagonizes 53BP1 dependent DNA end-blocking activity during S phase, which would otherwise promote mutagenic NHEJ and genome instability. Recently, it was shown that supra-physiological levels of the E3 ubiquitin ligase RNF168 results in the hyper-accumulation of 53BP1/BRCA1 which accelerates DSB repair. Here, we ask whether increased expression of RNF168 or 53BP1 impacts physiological versus mutagenic NHEJ. We find that the anti-resection activities of 53BP1 are rate-limiting for mutagenic NHEJ but not for physiological CSR. As heterogeneity in the expression of RNF168 and 53BP1 is found in human tumors, our results suggest that deregulation of the RNF168/53BP1 pathway could alter the chemosensitivity of BRCA1 deficient tumors.

INTRODUCTION

DSBs trigger ATM/ATR/DNA-PKcs-dependent phosphorylation of histone H2AX over a large chromatin domain, which serves as a molecular platform to concentrate downstream signaling and repair factors (1). Among the multitude of proteins that home to γH2AX-decorated chromatin are two RING-domain E3 ubiquitin ligases, RNF8 and RNF168 (2–6). Together, RNF8 and RNF168 catalyze a series of ubiquitylation events on substrates such as H2A and H2AX, with the $H2A^{K13/15}$ ubiquitylation being particularly important for subsequent relocation of 53BP1 into foci (7–9). Stable binding of 53BP1 to DNA ends channels DSB repair into non-homologous end joining (NHEJ) in part by suppressing end resection (10), a process that generates long stretches of single stranded DNA needed for HR. It has been proposed that BRCA1/CtIP excludes 53BP1 and/or its cofactors RIF1/PTIP from chromatin surrounding DSBs specifically in S-G_2 to allow extensive end resection, while in G_1, 53BP1 and its cofactor RIF1 blocks end resection (10–18). This ensures that HR is maximally activated only when sister chromatids are available to template faithful repair. In the absence of functional BRCA1, DNA lesions occurring in S-phase that are normally repaired through error-free HR are instead channeled into mutagenic NHEJ, resulting in the formation of highly aberrant end joining products such as chromosomal radials (10). Hence, BRCA1-deficiency confers exquisite sensitivity toward chemotherapeutic agents that damage DNA in S-phase cells, such as poly(ADP-ribose) polymerase inhibitors (PARPi) (10,19–20), whereas combined BRCA1/53BP1 deficiency rescues HR, resulting in resistance to PARPi.

Immunoglobulin (Ig) class switch recombination (CSR) is a physiological process in mature B cells that is critically dependent on the induction and repair of programmed DSBs in G_1 (21–23). CSR is initiated by activation-induced cytidine deaminase (AID), which generates multiple DSBs at highly repetitive Ig heavy chain switch regions (23–25). Rejoining of these DSBs requires 53BP1-dependent long-range NHEJ and replaces Igμ with a downstream constant region (Igγ, Igε or Igα) (26,27). Unlike mutagenic NHEJ, which inappropriately joins resected DSBs, physio-

*To whom correspondence should be addressed. Tel: +1 301 435 6425; Fax: +1 301 402 0711; Email: andre_nussenzweig@nih.gov

logical NHEJ reactions in the context of 53BP1-dependent CSR are typically more accurate wherein the majority of repair junctions show only minimal nucleotide changes. In the absence of 53BP1, however, AID-induced DSBs are resected in an ATM/CtIP-dependent manner and subsequently repaired by an alternative homology-driven pathway that generates non-productive intra-switch recombination (28–31). Notably, inhibition of ATM or CtIP activity partially enhanced CSR in 53BP1-deficient B cells, suggesting that end resection is an important negative regulator of NHEJ that must be suppressed by 53BP1 to enable efficient CSR (29,30).

RNF168 is a key upstream regulator of 53BP1 and was reported to be critical for the HR defects caused by BRCA1 deficiency (32–34), suggesting that RNF168 inhibits resection by controlling 53BP1 recruitment to DNA damage sites. In addition, RNF168 promotes CSR (35,36). Recently, it was found that RNF168 stabilization led to augmented 53BP1 spreading and accelerated repair of clastogen-induced DSBs (37). This raises the possibility that DSB repair during mutagenic NHEJ in S phase and/or physiological CSR in G_1 can be similarly enhanced by increasing the expression of RNF168 and/or 53BP1. Here, we demonstrate that amplification of 53BP1 spreading has deleterious consequences for genome stability during S phase yet does not influence NHEJ during CSR. Thus, the requirements for DNA damage-induced histone ubiquitylation during NHEJ-mediated CSR and misrepair of PARPi-induced DNA damage are distinct. Finally, given the heterogeneous expression of RNF168 and 53BP1 in BRCA1-deficient tumors, our data may have therapeutic implications for PARPi treatment and predicting tumor responses.

MATERIALS AND METHODS

Mice

$BRCA1^{f(\Delta 11)/f(\Delta 11)}$ (NCI mouse repository) and $BRCA1^{f(\Delta 11)/f(\Delta 11)}/53BP1^{-/-}$ (10) mice have been described. All experiments with mice followed protocols approved by the National Institutes of Health Institutional Animal Care and Use Committee.

Cell cultures, retroviral infection and flow cytometry

Wild-type, $BRCA1^{\Delta 11/\Delta 11}$, $53BP1^{-/-}$ and $BRCA1^{\Delta 11/\Delta 11}53BP1^{-/-}$ mouse embryonic fibroblasts (MEFs) have been described (10). Resting B cells were isolated from spleen using anti-CD43 microbeads (Miltenyi Biotec) and stimulated to proliferate with 25 μg/ml LPS, 5 ng/ml IL-4 (both Sigma-Aldrich) and 0.5 μg/ml RP105 (BD PharMingen) (10). To overexpress RNF168, constructs encoding human $RNF168^{WT}$ or $RNF168^{R57D}$ (9) were subcloned into the pMX-PIE-IRES-GFP retroviral vector and used to transfect BOSC23 cells along with the pCL-Eco helper virus. Retroviral supernatant was collected 40–48 h later for infection of MEFs and B cells as previously described (38). pMX-PIE-based retroviruses encoding $53BP1^{DB}$ and $53BP1^{DN}$ have been described (11,28). Class switch recombination was assayed on days 3 and 4 using biotinylated anti-IgG$_1$ and fluorochrome-conjugated anti-B220 antibodies (BD PharMingen).

FISH analysis

Stimulated B cells and MEFs were arrested at mitosis with colcemid (Invitrogen) treatment and harvested for metaphase spreads as described (38). Images were captured with an automated fluorescence microscope (Axio Imager Metasystems; Zeiss). One hundred metaphases were scored for the presence of chromosomal aberrations.

Cell cycle analysis

Cells were fixed in 70% ethanol and stained with propidium iodide for flow cytometric analysis. ModFit LT (Verity Software House) was used to assign cell cycle distribution.

Colony formation and growth competition assays

MEFs were treated with 1 μM PARPi (KU-0058948, Axon Medchem) either continuously for 10 days (wild-type, $53BP1^{-/-}$) or for 24 h followed by a 9-day post-incubation in drug-free medium ($BRCA1^{\Delta 11/\Delta 11}$). Thereafter, culture dishes were stained with 0.5% crystal violet and colonies containing >50 cells were counted. Due to poor colony forming ability of $BRCA1^{\Delta 11/\Delta 11}53BP1^{-/-}$ MEFs, a growth competition assay was used instead. To this end, $BRCA1^{\Delta 11/\Delta 11}53BP1^{-/-}$ MEFs stably transduced with retroviral vectors encoding $RNF168^{WT}$ or $RNF168^{R57D}$ (GFP-positive) were mixed with non-transduced $BRCA1^{\Delta 11/\Delta 11}53BP1^{-/-}$ MEFs (GFP-negative) at a 1:1 ratio. Alternatively $BRCA1^{\Delta 11/\Delta 11}53BP1^{-/-}$ MEFs stably transduced with retroviral vectors encoding $53BP1^{DB}$ (GFP-negative) were mixed with $BRCA1^{\Delta 11/\Delta 11}53BP1^{-/-}$ MEFs stably transduced with the empty vector (GFP-positive). Cells were treated or not with 1 μM PARPi continuously for 9 days. Samples were collected before (day 0) as well as after PARPi treatment on days 1, 3, 5, 7 and 9 for flow cytometric analysis. Relative proliferation was calculated by normalizing the fraction of GFP-positive cells in PARPi-treated versus untreated samples collected on the same day.

Immunofluorescence

For standard immunofluorescence studies, MEFs grown on coverslips were subjected to γ-irradiation (cesium-137) or treated with PARPi. At the indicated times post-treatment, cells were first pre-extracted (20 mM HEPES, pH 7.0, 50 mM NaCl, 3 mM MgCl$_2$, 0.3 M sucrose, 0.2% Triton X-100) for 5 min on ice to remove nucleoplasmic proteins and then sequentially fixed (4% paraformaldehyde), permeabilized (0.5% Triton X-100) and blocked (2% BSA). Samples were incubated with primary antibodies recognizing HA-tag (Santa Cruz Biotechnology), RNF168 (Millipore), conjugated ubiquitin (FK2, Sigma–Aldrich), 53BP1 (Novus Biologicals), RIF1 (14), RPA2 (Cell Signaling Technologies), RAD51 (H-92; Santa Cruz Biotechnology) followed by appropriate fluorochrome-conjugated secondary antibodies (Invitrogen). DNA was counterstained with DAPI. Foci images were captured with a fluorescence microscope at 63× magnification, unless otherwise stated. High-throughput automated imaging was used to captured chromatin-bound RPA at 20× magnification. Integrated nuclear RPA intensity was quantified using CellProfiler 2.0.
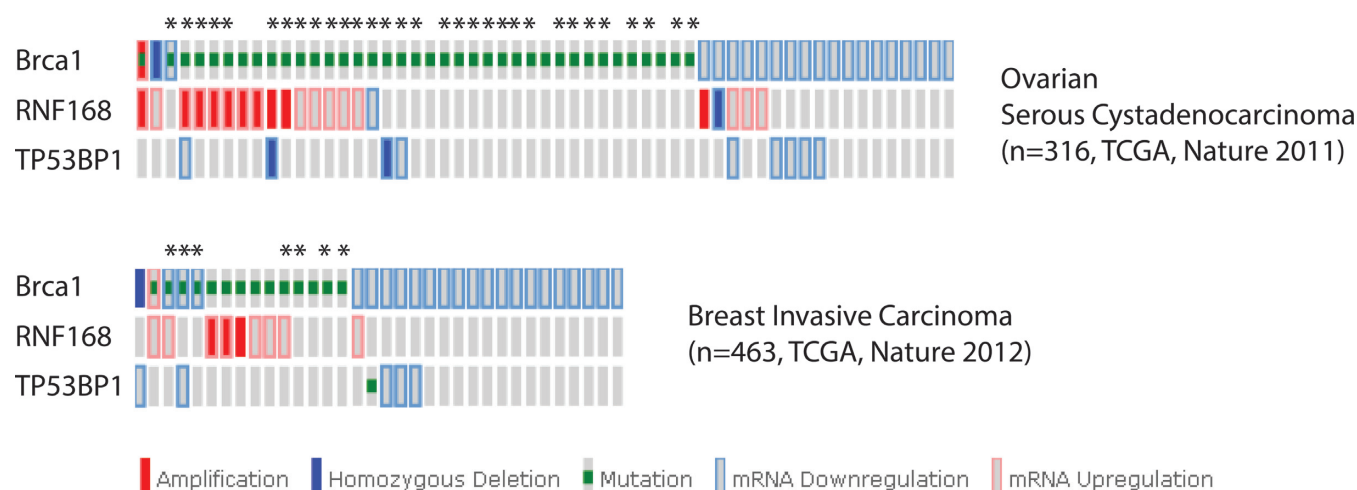
Figure 1. The RNF168/53BP1 pathway is altered in a subset of BRCA1-deficient tumors. Mutation data for two TCGA studies were extracted from cBioPortal (www.cbioportal.org) and used to generate oncoprints showing examples of RNF168/53BP1 pathway heterogeneity in BRCA1-deficient tumors (39–58). Asterisks denote tumors where BRCA1 is mutated in one allele and deleted in the other. All other BRCA1-mutated tumors contain heterozygous germline mutations.

Immunoblotting

Whole cell extract (WCE) was resolved by SDS-PAGE (NuPAGE, Invitrogen) and transferred onto nitrocellulose membranes. Samples were incubated with primary antibodies recognizing RNF168 (Millipore), 53BP1 (Novus Biologicals), phospho-RPA2 (S4, S8), phospho-CHK1 (S317; all from Bethyl Laboratories), RPA2 (Cell Signaling Technologies) and α-tubulin (Sigma–Aldrich). Following incubation with the appropriate horseradish peroxidase-linked secondary antibodies (GE Healthcare), bands were visualized using enhanced chemiluminescence (GE Healthcare).

RESULTS

RNF168 and 53BP1 levels modulate PARP inhibitor-induced genome instability in BRCA1 deficient cells

53BP1 has been shown to promote mutagenic NHEJ in BRCA1-deficient cells by blocking end resection, which leads to PARPi hypersensitivity and tumorigenesis (10). For both 53BP1 and its immediate upstream regulator RNF168 we found copy number variations, genetic mutations and/or heterogeneous mRNA expression changes in a subset of BRCA1-deficient ovarian and breast tumors within the TCGA database (39–42(Figure 1). We therefore sought to determine whether modulating the chromatin loading of RNF168 and/or 53BP1 would alter PARPi sensitivity. To this end, we established mouse embryonic fibroblast (MEF) cell lines transduced with retroviral vectors encoding either wild-type RNF168 (RNF168^{WT}) or a RNF168 mutant (RNF168^{R57D}) that is incapable of 53BP1 recruitment (9) (Figure 2, Supplementary Figures S1A and Supplementary Figure S2). Since efficient transduction of MEFs with wild-type 53BP1 proved to be difficult due to its large size, we chose instead to overexpress 53BP1^{DB}, a construct that lacks the extreme C-terminal BRCT domain but behaves like wild-type 53BP1 in terms of DSB end-protection (28), or a dominant negative fragment of 53BP1 (53BP1^{DN}) (43) (Supplementary Figure S1B and C). As reported by

Gudjonsson *et al.* (37), we found that overexpression of RNF168^{WT} in BRCA1$^{\Delta11/\Delta11}$ MEFs promoted the formation of conjugated ubiquitin and 53BP1 as well as RIF1 foci upon DNA damage caused by PARP inhibition or ionizing radiation (Figure 3A and Supplementary Figure S2). Interestingly, enlarged 53BP1 foci were also observed in BRCA1$^{\Delta11/\Delta11}$ MEFs overexpressing 53BP1^{DB} (Figure 4B). Thus, overexpression of 53BP1 itself can bypass the control of its spreading on damaged chromatin, which is normally limited by the availability of RNF168.

While PARPi treatment already caused substantial genome instability in BRCA1$^{\Delta11/\Delta11}$ control cells (MEFs infected with an empty vector), PARPi-induced genome instability was further increased by 1.5–2-fold following overexpression of RNF168^{WT} or 53BP1^{DB} (Figure 3B and C). Conversely, BRCA1$^{\Delta11/\Delta11}$ MEFs overexpressing RNF168^{R57D} or 53BP1^{DN} had less PARPi-induced chromosomal aberrations than control cells, although in the case of RNF168^{R57D} the difference did not reach statistical significance (Figure 3B and C). Consistent with these observations, overexpression of RNF168^{WT} or 53BP1^{DB} conferred PARPi hypersensitivity in BRCA1$^{\Delta11/\Delta11}$ MEFs in a colony formation assay whereas overexpression of RNF168^{R57D} or 53BP1^{DN} partially rescued long-term clonogenic survival (Figure 3D). Taken together, these data show that the level of chromatin-bound RNF168 and 53BP1 dictates the extent of PARPi-induced genome instability and long-term survival in BRCA1-deficient cells. Therefore, we propose that excessive spreading of either endogenous 53BP1 brought on by increased RNF168-mediated H2A ubiquitylation or its exogenously overexpressed counterpart 53BP1^{DB}, impedes HR.

RNF168 and 53BP1 antagonize long-range end resection and RPA phosphorylation in BRCA1-deficient cells

BRCA1-mediated removal of 53BP1 is thought to be an essential prerequisite for end resection and RAD51-dependent HR (12,14–16,18). In agreement with
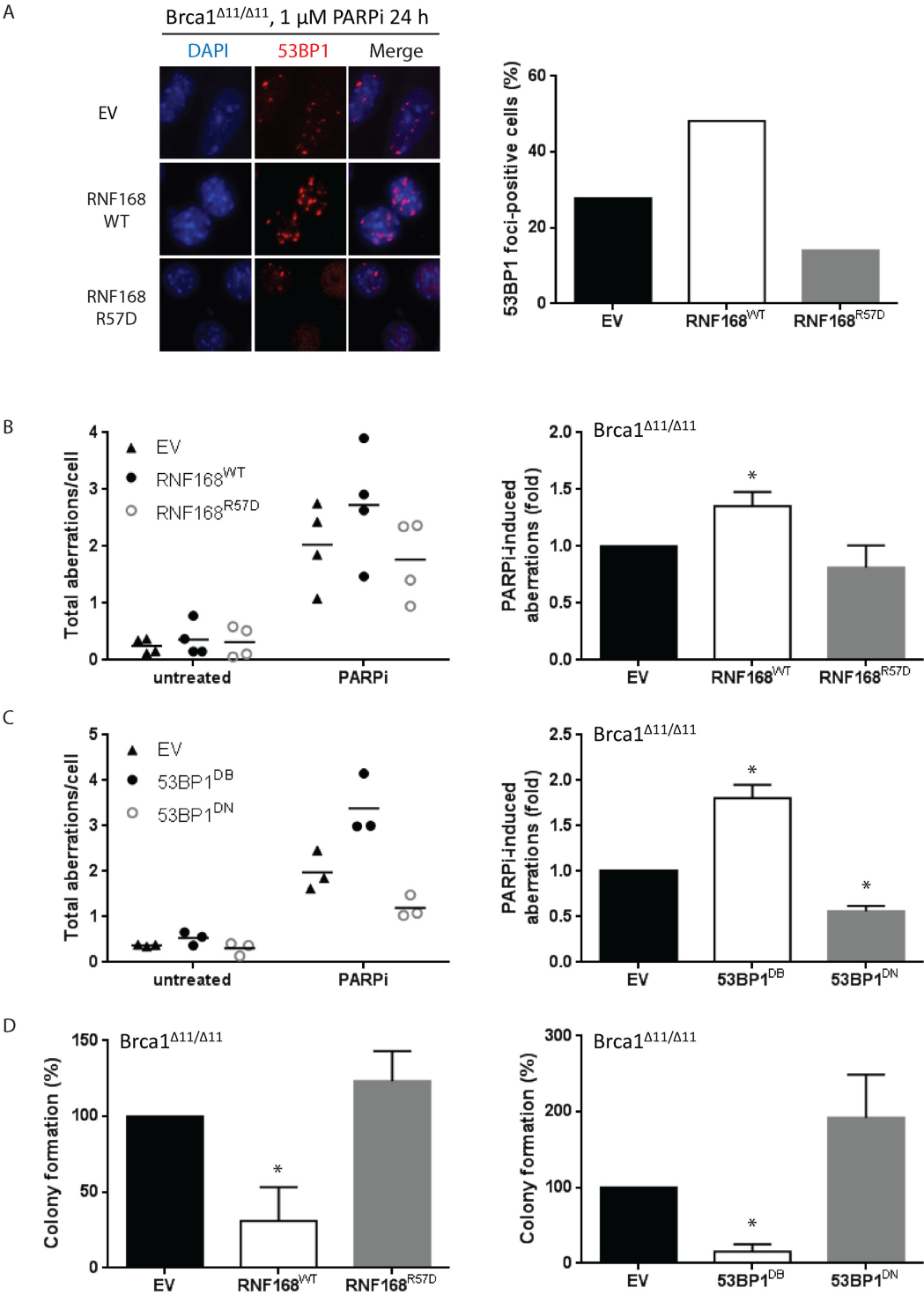
Figure 2. Schematic depiction of the retroviral vectors used in this study. (**A**) The RNF168[WT] and RNF168[R57D] differ in their ability to specifically interact with and ubiquitylate histone H2A due to a point mutation in the RING domain. MIU, motif interacting with ubiquitin. (**B**) 53BP1[DB] lacks the C-terminal BRCT domain present in full-length 53BP1 while 53BP1[DN] consists only of the minimal region required for foci formation. 53BP1[DB] is functionally wild-type with respect to end-protection and CSR (28), whereas 53BP1[DN] acts as a dominant negative mutant. OD, oligomerization domain; UDR, ubiquitylation-dependent recruitment.

this, 53BP1[DB] suppressed RAD51 foci formation in BRCA1[$\Delta 11/\Delta 11$] MEFs (Supplementary Figure S3A). End resection enables RPA to form foci along progressively longer stretches of single-stranded DNA (ssDNA) before it is actively displaced by RAD51 (44). A recent report found that end resection can occur in the absence of functional BRCA1 but the process is slower and less efficient (45). Notably, overexpression of either RNF168[WT] or 53BP1[DB]

in irradiated BRCA1[$\Delta 11/\Delta 11$] MEFs further suppressed the chromatin loading of RPA compared to control cells (Figure 4A, B and Supplementary Figure S3B). Importantly, the cycling of BRCA1[$\Delta 11/\Delta 11$] MEFs was not affected by overexpression of RNF168 or 53BP1, thus ruling out the possibility that differences in cell cycle progression contributed to the observed differences in RPA foci formation (Supplementary Figure S4). DNA-PK-dependent RPA2

Figure 3. Overexpression of RNF168 or 53BP1 exacerbates PARP inhibitor-induced genomic instability and cytotoxicity. (**A**) BRCA1$^{\Delta 11/\Delta 11}$ cells were treated with 1 μM PARPi for 24 h and processed for standard immunofluorescence. Left panel: cells were stained for 53BP1 (red) and imaged at 63× magnification. A representative experiment is shown. Right panel: the percentage of cells that contain >5 foci of 53BP1 from two independent experiments. At least 200 cells were scored for each sample and treatment condition. (**B**) BRCA1$^{\Delta 11/\Delta 11}$ MEFs stably transduced with retroviral vectors encoding RNF168^{WT} or RNF168^{R57D} were treated with 1 μM PARPi (24 h) and harvested for preparation of metaphase spreads. Left panel: dot plots indicating the total amount of aberrations per cell in four independent experiments. At least 100 metaphases were analyzed for each condition. Right panel: histograms depicting PARPi-induced chromosomal aberration load relative to empty vector-transduced cells for the same experiments as shown in the corresponding left panels. (**C**) Similar to (B), except in BRCA1$^{\Delta 11/\Delta 11}$ MEFs stably transduced with retroviral vectors encoding 53BP1^{DB} or 53BP1^{DN}. (**D**) Cells were treated with 1 μM PARPi for 24 h and then incubated in drug-free medium to allow formation of colonies. After 9 days, culture dishes were stained with crystal violet and colonies containing >50 cells were counted. Results are mean ± SD of three independent experiments. For (A)–(D), Statistical significance was determined with two-tailed unpaired Student's *t*-test; *, $P < 0.05$ compared to empty vector-transduced cells.
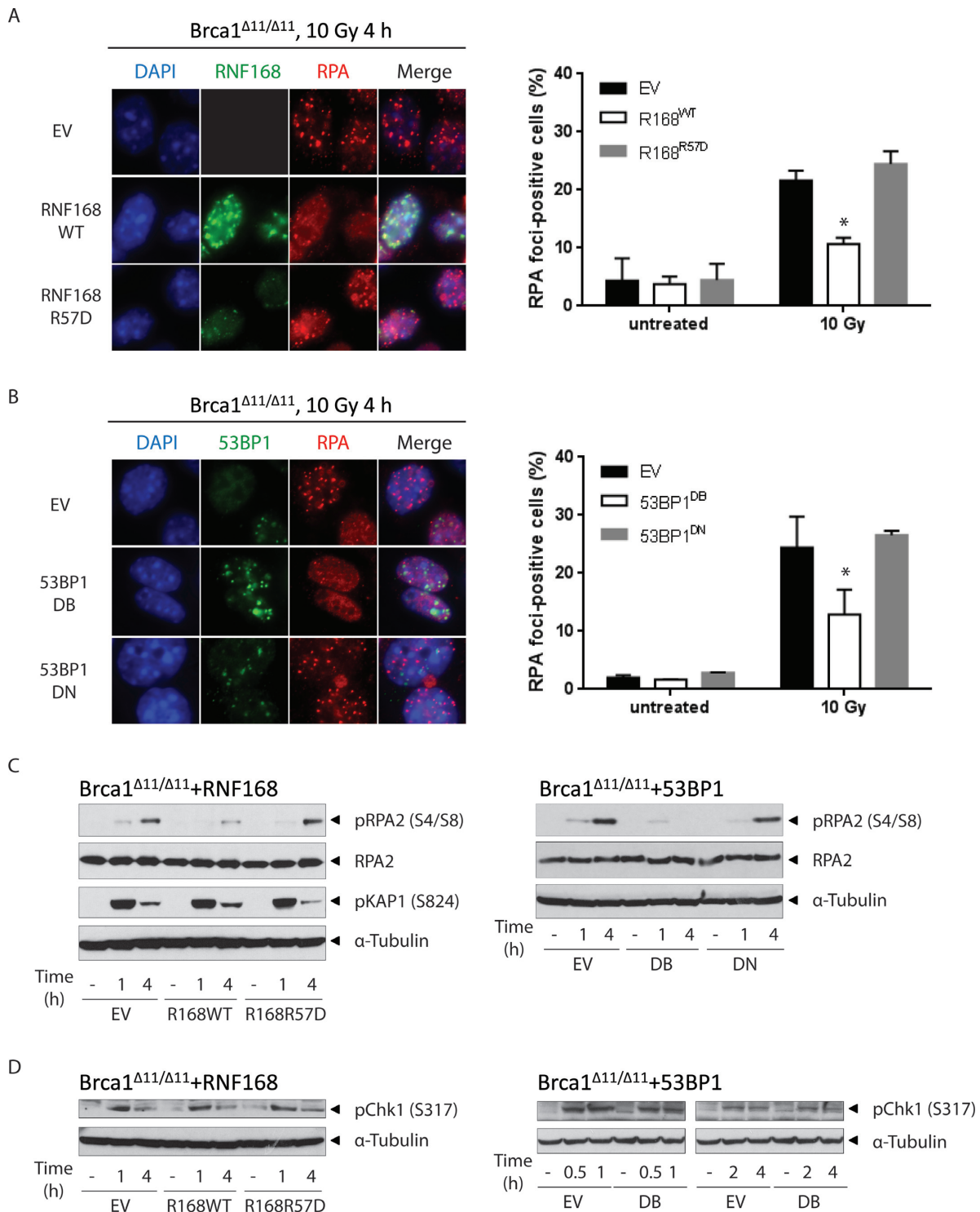
Figure 4. RNF168 and 53BP1 block RPA foci formation and RPA2 phosphorylation. (**A**) BRCA1$^{\Delta11/\Delta11}$ MEFs stably transduced with retroviral vectors encoding RNF168^{WT} or RNF168^{R57D} were irradiated with 10 Gy and fixed 4 h later. Samples were processed for standard immunofluorescence. Left panel: cells were co-stained for RNF168 (green) and RPA2 (red) and imaged at 63× magnification. Note that the polyclonal anti-RNF168 antibody used in this study recognizes only the exogenously expressed human RNF168. A representative experiment is shown. Right panel: the percentage of cells that contain >10 RPA2 foci. (**B**) BRCA1$^{\Delta11/\Delta11}$ MEFs stably transduced with retroviral vectors encoding 53BP1^{DB} or 53BP1^{DN} were irradiated and processed for standard immunofluorescence as in (A). Left panel: cells were co-stained for 53BP1 (green) and RPA2 (red) and imaged at 63x magnification. A representative experiment is shown. Right panel: the percentage of cells that contain >10 RPA2 foci. The right panels in A and B show mean ± SD of three independent experiments. At least 200 cells were scored for each sample and treatment condition. (**C**) Similar to (A), except cells were harvested at the indicated post-irradiation time points for western blot analysis. (**D**) Similar to (B), except cells were harvested at the indicated post-irradiation time points for western blot analysis. A representative blot is shown in (C) and (D). Experiments were repeated three times. For (A) and (B), statistical significance was determined with two-tailed unpaired Student's *t*-test; *, $P < 0.05$ compared to empty vector-transduced cells.
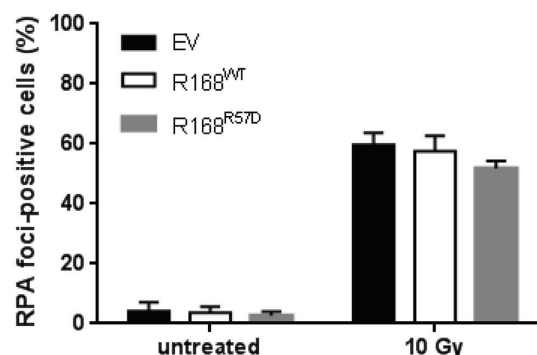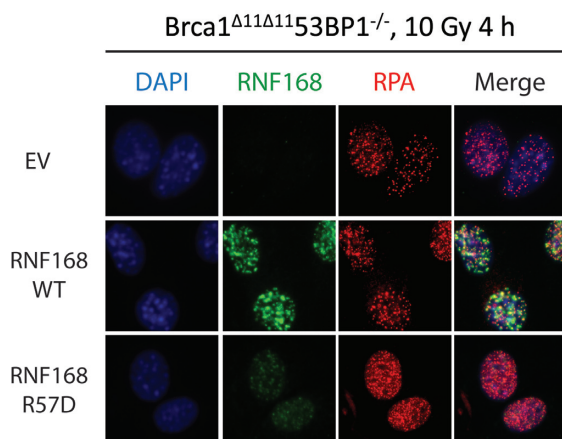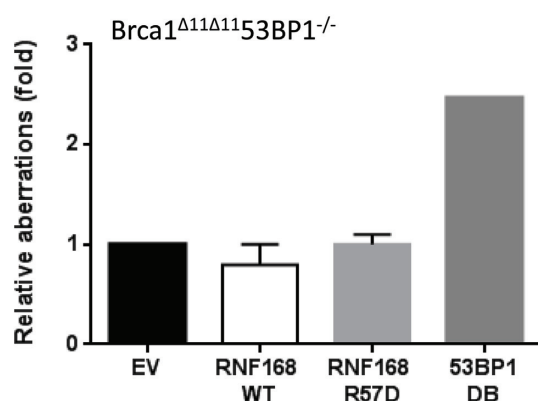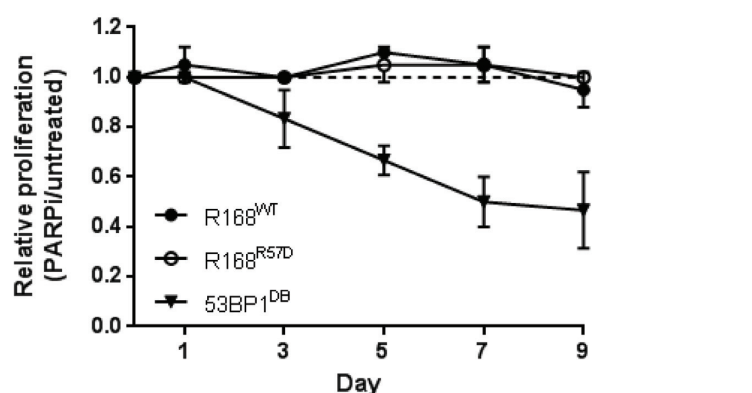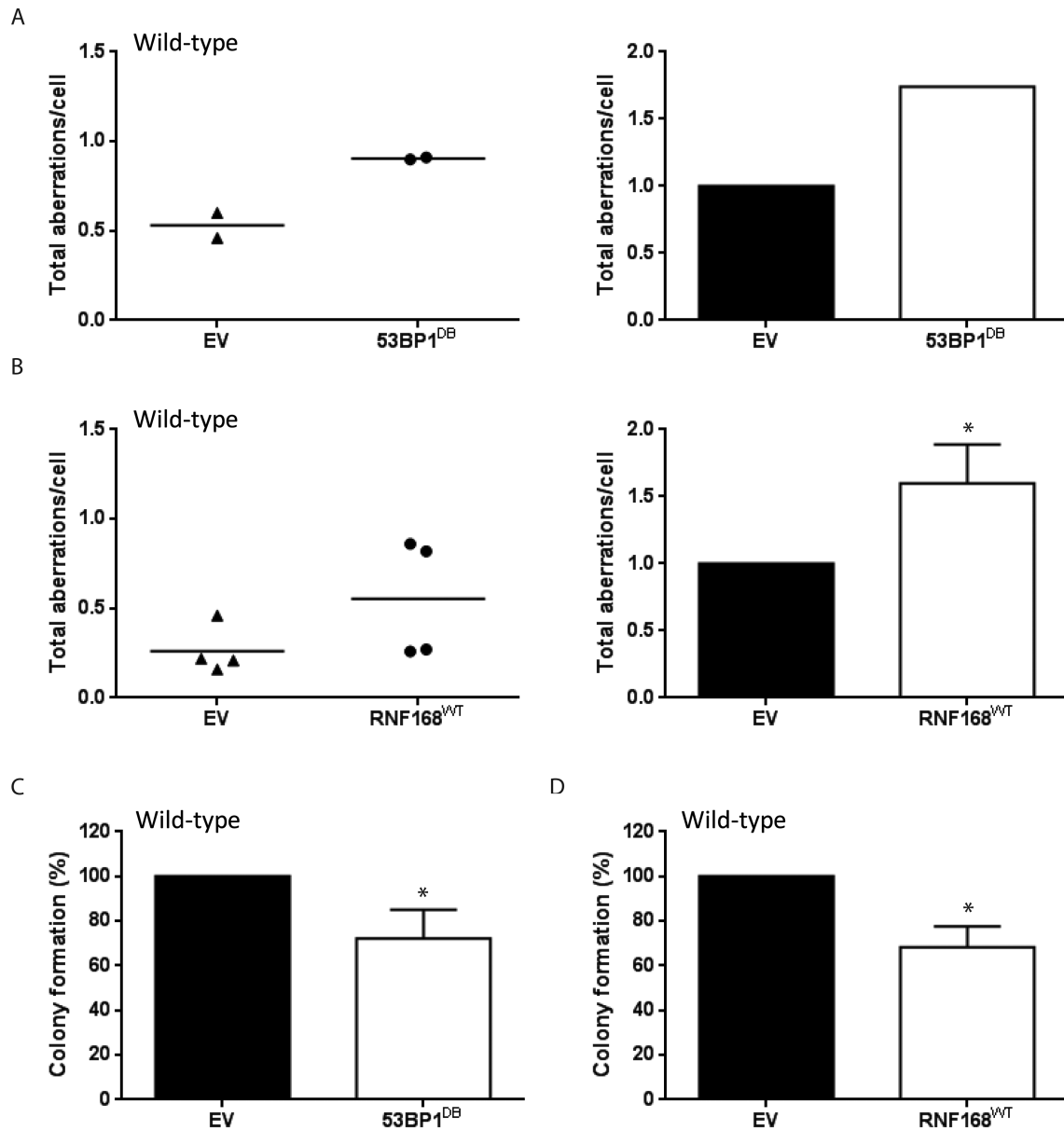
Figure 5. RNF168 uses 53BP1 to block RPA loading in BRCA1-deficient cells. (**A**) BRCA1$^{\Delta11/\Delta11}$53BP1$^{-/-}$ MEFs stably transduced with retroviral vectors encoding RNF168^{WT} or RNF168^{R57D} were irradiated with 10 Gy and fixed 4 h later. Samples were processed for standard immunofluorescence. Left panel: cells were co-stained for RNF168 (green) and RPA2 (red) and imaged at 20x magnification (optovar: 1.25×). A representative experiment is shown. Right panel: the percentage of cells that contain >10 RPA2 foci. At least 100 cells were scored for each sample and treatment condition. (**B**) BRCA1$^{\Delta11/\Delta11}$53BP1$^{-/-}$ MEFs stably transduced with retroviral vectors encoding RNF168^{WT}, RNF168^{R57D} or 53BP1^{DB} were treated with 1 µM PARPi (24 h) and harvested for preparation of metaphase spreads. Histograms depict PARPi-induced chromosomal aberration load relative to empty vector-transduced cells for two-three independent experiments. At least 100 metaphases were analyzed for each condition. (**C**) BRCA1$^{\Delta11/\Delta11}$53BP1$^{-/-}$ MEFs stably transduced with retroviral vectors encoding RNF168^{WT} or RNF168^{R57D} (GFP-positive) were plated with non-transduced BRCA1$^{\Delta11/\Delta11}$53BP1$^{-/-}$ MEFs (GFP-negative) at a 1:1 ratio. Alternatively BRCA1$^{\Delta11/\Delta11}$53BP1$^{-/-}$ MEFs stably transduced with retroviral vectors encoding 53BP1^{DB} (GFP-negative) were mixed 1:1 with BRCA1$^{\Delta11/\Delta11}$53BP1$^{-/-}$ MEFs stably transduced with the empty vector (GFP-positive). Cells were treated or not with 1 µM PARPi continuously for 9 days. Samples were collected before (day 0) as well as after PARPi treatment on days 1, 3, 5, 7 and 9 for flow cytometric analysis. Relative proliferation is calculated by normalizing the fraction of GFP-positive cells in PARPi-treated versus untreated samples collected on the same day. Data shown represents mean ± SD of three independent experiments.

(S4, S8) phosphorylation was also significantly attenuated in BRCA1$^{\Delta11/\Delta11}$ MEFs overexpressing RNF168^{WT} or 53BP1^{DB} (Figure 4C). In contrast the phosphorylation of KAP-1, an ATM substrate that responds to DSBs, remained unchanged (Figure 4C). Interestingly, ATR-mediated phosphorylation of CHK1 was not perturbed by RNF168^{WT} or 53BP1^{DB} overexpression (Figure 4D). Since CHK1 activation by ATR requires only minimal resection (46,47), these results suggest that RNF168 regulates 53BP1 chromatin binding to antagonize long-range DSB end resection in BRCA1-deficient cells. Consistent with this notion, RNF168^{WT} failed to block RPA loading (Figure 5A) or to enhance PARPi sensitivity in BRCA1$^{\Delta11/\Delta11}$

MEFs when 53BP1 was co-deleted (Figure 5B and C). By contrast, 53BP1^{DB} overexpression re-imparted susceptibility to PARPi-induced genome instability and decreased the survival of BRCA1$^{\Delta11/\Delta11}$53BP1$^{-/-}$ MEFs (Figure 5B and C).

In wild-type and 53BP1$^{-/-}$ MEFs, where BRCA1 is fully operational, ectopic expression of 53BP1^{DB} also led to increased genome instability in response to PARPi treatment (Figure 6A and Supplementary Figure S1D). Moreover, 53BP1^{DB} suppressed RAD51 loading in wild-type MEFs, as evidenced by the reduced numbers and smaller sizes of RAD51 foci (Supplementary Figure S3C), although this effect was milder than in BRCA1-deficient MEFs. As a re-
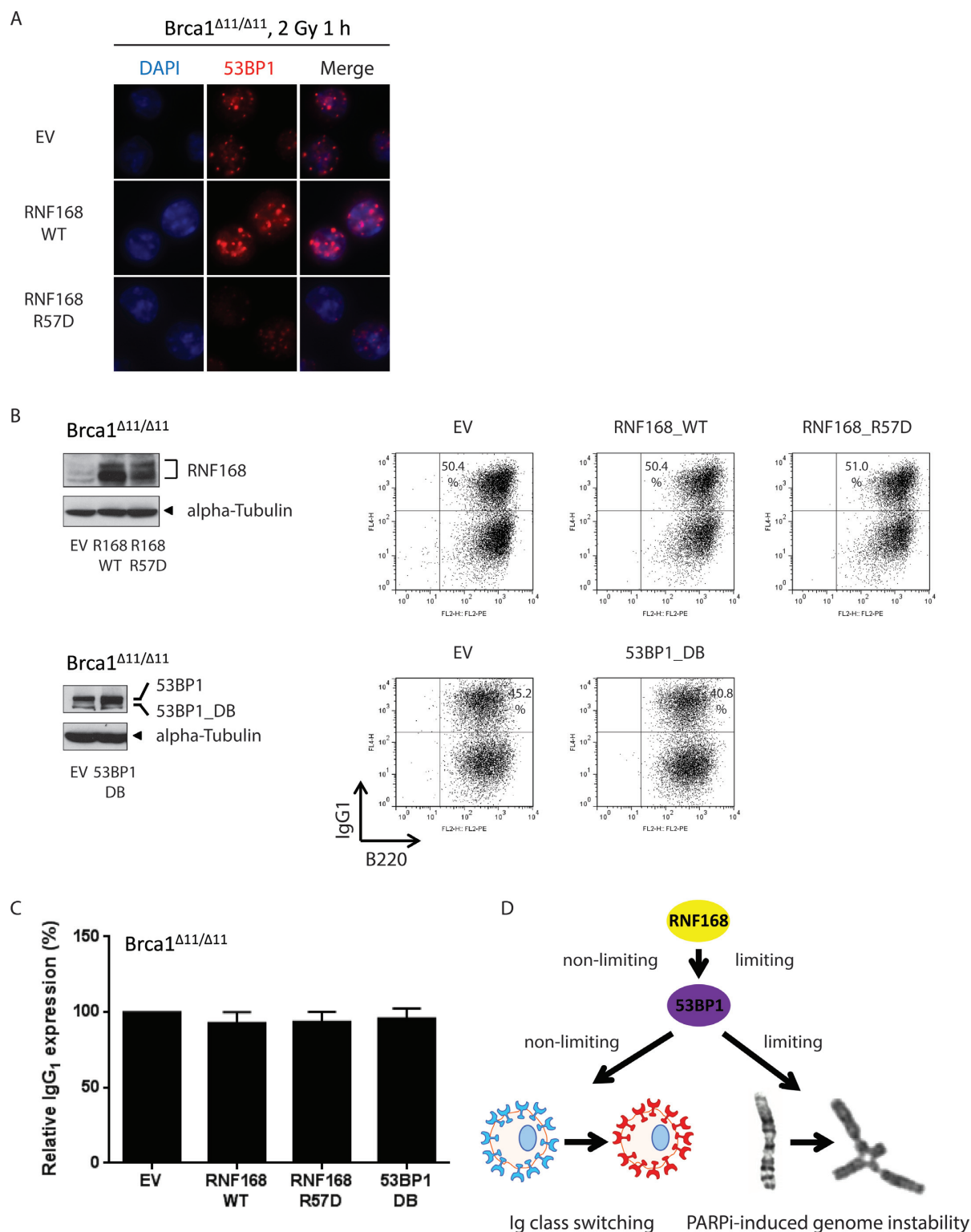
Figure 6. 53BP1 suppresses HR in wild-type cells. Wild-type cells were stably transduced with retroviral vectors encoding 53BP1^{DB} or RNF168^{WT}. (**A**, **B**) Cells were treated with 1 μM PARPi (24 h) and harvested for preparation of metaphase spreads. Left panels: dot plots indicating the total amount of aberrations per cell. Right panels: histograms depict PARPi-induced chromosomal aberration load relative to empty vector-transduced cells. At least 100 metaphases were scored for chromosomal aberrations for each condition. Results are mean ± SD of two (**A**) and four (**B**) independent experiments, respectively. (**C**, **D**) Cells were treated with 1 μM PARPi continuously for 10 days, after which culture dishes were stained with crystal violet and colonies containing >50 cells were counted. Results are mean ± SD of three independent experiments. For (**B**), (**C**) and (**D**), statistical significance was determined with two-tailed unpaired and paired Student's *t*-test, respectively; *$P < 0.05$ compared to empty vector-transduced cells.

sult, 53BP1^{DB} overexpression partially enhanced the toxicity of PARPi in wild-type MEFs (Figure 6A and C). Similarly, overexpression of RNF168^{WT} increased PARPi-induced genome instability and cytotoxicity in wild-type MEFs (Figure 6B and D). Taken altogether, our data suggest that while a functional BRCA1 pathway can fully counteract endogenous RNF168/53BP1 during a normal S-phase DNA damage response, increased levels of RNF168 and 53BP1 can still suppress HR, increase toxicity and limit long-range end resection in BRCA1-proficient cells.

RNF168 and 53BP1 are not limiting factors during immunoglobulin class switch recombination

53BP1 promotes productive long-range NHEJ during CSR and VDJ recombination at least in part by blocking end resection (11,26–28,31,48). A recent study found that increased 53BP1 spreading caused by stabilization of RNF168 accelerates NHEJ (37); we therefore asked whether overexpression of exogenous RNF168 and/or 53BP1 might augment CSR. However, overexpression of RNF168 or 53BP1 did not affect CSR in wild-type B cells (Supplementary Figure S5). Next, we tested whether ex-

Figure 7. RNF168 and 53BP1 are not limiting factors during immunoglobulin class switch recombination (CSR). (**A**) BRCA1$^{\Delta11/\Delta11}$ splenic B cells transduced with retroviral vectors encoding RNF168^{WT} or RNF168^{R57D} were cultured in the presence of LPS/IL-4/RP105 to stimulate CSR. On day 3, cells were irradiated with 2 Gy and fixed 1 h later. Samples were stained for 53BP1 (red) and imaged at 63× magnification. (**B**) BRCA1$^{\Delta11/\Delta11}$ splenic B cells were transduced with retroviral vectors encoding RNF168^{WT}, RNF168^{R57D} or 53BP1^{DB} and cultured in the presence of LPS/IL-4/RP105 to stimulate CSR. Left panels: overexpression of RNF168 and 53BP1 were confirmed by western blotting. The upper band in the 53BP1 blot corresponds to the endogenous protein. Right panels: two-color flow cytometric analysis of IgG$_1$ expression in B220-positive cells on day 4; scatter plots for B cells overexpressing RNF168 and its empty vector counterpart were gated on GFP. A representative experiment is shown. (**C**) Frequency of IgG$_1$ expression in B220-positive BRCA1$^{\Delta11/\Delta11}$ B cells from three-four independent experiments. (**D**) Model depicting the differential roles of 53BP1 and RNF168 in physiological and mutagenic NHEJ.

ogenous RNF168 and/or 53BP1 might augment CSR in the context of a resection defect imparted by BRCA1 deficiency. As expected (37), retroviral-mediated overexpression of RNF168^{WT} led to enhanced chromatin loading of 53BP1 (Figure 7A). Despite this, however, overexpression of RNF168^{WT} or 53BP1^{DB} did not significantly enhance CSR in BRCA1-deficient B cells (Figure 7B and C). Conversely, CSR was not reduced by enforced expression of RNF168^{R57D} (Figure 7B and C). Together, these data demonstrate that levels of chromatin-bound 53BP1 are not rate-limiting for physiological NHEJ during CSR (Figure 7D).

DISCUSSION

End resection is a key determinant of DSB repair choice in mammalian cells (44). It peaks in the S-G$_2$ phase of the cell cycle, when sister chromatids are available to template error-free repair by HR, but is actively suppressed by 53BP1 in G$_1$, where HR would be harmful (49–51). A critical function of BRCA1 during S phase is to exclude 53BP1 and its cofactors from chromatin surrounding DSBs allowing long-range resection by nucleases (12–13,15). Loss of BRCA1, which occurs in a significant proportion of human ovarian and breast cancers, allows 53BP1 to aberrantly accumulate at DSB sites in S-G$_2$ and block resection, thereby impairing HR and shifting the repair of replication-associated DSBs into error-prone NHEJ, leading to the formation of toxic repair intermediates and tumorigenesis (10,52). As such, BRCA1-deficient tumors are exquisitely sensitive to treatment with drugs that induce DSBs in S-phase, such as PARPi (19). Conversely, loss of 53BP1 expression has been implicated as a potential mechanism of acquired resistance to PARPi in BRCA1-deficient tumors (53–55). We found that a subset of BRCA1-deficient tumors within the TCGA database show copy number variation, mutation and/or mRNA expression changes in RNF168 or 53BP1 (Figure 1). Moreover, we have shown that overexpression of RNF168 or 53BP1^{DB} confers PARPi hypersensitivity in BRCA1$^{\Delta11/\Delta11}$ cells by promoting 53BP1 spreading and further suppressing the already sub-optimal resection machinery (Figures 3 and 4). These data indicate that heterogeneity in the RNF168/53BP1 pathway can be an important and therapeutically relevant modifier of chemosensitivity in BRCA1-deficient tumors.

Deregulation of the RNF168/53BP1 pathway is not limited to BRCA1-deficient tumors. For ovarian and breast cancers that are wild-type for BRCA1, elevated expression of 53BP1 is associated with decreased survival and lymph node metastasis, respectively (56,57). A possible scenario is that increased expression of 53BP1 *per se* promotes genome instability by compromising the ability of HR to overcome replication stress in rapidly cycling tumor cells. Consistent with this, we found that overexpression of 53BP1 enhanced the accumulation of chromosomal aberrations in wild-type MEFs and led to a mild decrease in colony formation after PARPi treatment (Figure 6). However, PARPi-induced cytotoxicity was more severe in BRCA1-deficient cells relative to wild-type when 53BP1 was overexpressed (compare Figures 3D and 6C). This is presumably because the extent of damage in absolute terms is still relatively low and can

thereby be tolerated in wild-type cells. Our data therefore suggest that tumors with functional BRCA1 and elevated RNF168/53BP1 levels may derive only limited benefit from PARPi-based therapy. Nevertheless, 53BP1 overexpression can increase mutagenic NHEJ by suppressing HR in both WT and BRCA1-deficient cells.

We found that the requirements of 53BP1 in mutagenic repair of PARPi-induced DNA damage and physiological NHEJ during CSR are dissimilar (Figure 7D). As it has been proposed that the anti-resection function of 53BP1 is critical for CSR (28–29,31), we reasoned that further inhibiting end resection with exogenously overexpressed 53BP1 might lead to enhanced CSR. To our surprise, however, neither RNF168 nor 53BP1 had any significant impact on CSR efficiency when overexpressed. Therefore, the expression levels of RNF168 or 53BP1 proteins are clearly more than sufficient to handle all AID-generated breaks under physiological conditions. Since the levels of RNF168 render ubiquitin signaling rate-limiting when the number of DSBs exceeds 20–40 (37), one possible explanation for these findings is that PARPi-induced DSBs in BRCA1-deficient cells may far exceed the number of DSBs generated by AID during CSR. The increased DSBs in PARPi-treated cells, in contrast to the fewer number of CSR-associated breaks could saturate histone ubiquitylation. To date, the only known limiting factor for CSR is AID itself (58), which when overexpressed causes supra-physiological accumulation of cleavage events at Ig switch regions, additional substrates for 53BP1-dependent NHEJ and increased CSR. Taken together, these data showed that the anti-resection activity of 53BP1 is limiting during mutagenic but not physiological NHEJ.

SUPPLEMENTARY DATA

Supplementary Data are available at NAR Online.

REFERENCES

1. Matsuoka,S., Ballif,B.A., Smogorzewska,A., McDonald,E.R. 3rd, Hurov,K.E., Luo,J., Bakalarski,C.E., Zhao,Z., Solimini,N., Lerenthal,Y. *et al.* (2007) ATM and ATR substrate analysis reveals extensive protein networks responsive to DNA damage. *Science*, **316**, 1160–1166.
2. Doil,C., Mailand,N., Bekker-Jensen,S., Menard,P., Larsen,D.H., Pepperkok,R., Ellenberg,J., Panier,S., Durocher,D., Bartek,J. *et al.* (2009) RNF168 binds and amplifies ubiquitin conjugates on damaged chromosomes to allow accumulation of repair proteins. *Cell*, **136**, 435–446.

3. Huen,M.S., Grant,R., Manke,I., Minn,K., Yu,X., Yaffe,M.B. and Chen,J. (2007) RNF8 transduces the DNA-damage signal via histone ubiquitylation and checkpoint protein assembly. *Cell*, **131**, 901–914.

4. Kolas,N.K., Chapman,J.R., Nakada,S., Ylanko,J., Chahwan,R., Sweeney,F.D., Panier,S., Mendez,M., Wildenhain,J., Thomson,T.M. *et al.* (2007) Orchestration of the DNA-damage response by the RNF8 ubiquitin ligase. *Science*, **318**, 1637–1640.

5. Mailand,N., Bekker-Jensen,S., Faustrup,H., Melander,F., Bartek,J., Lukas,C. and Lukas,J. (2007) RNF8 ubiquitylates histones at DNA double-strand breaks and promotes assembly of repair proteins. *Cell*, **131**, 887–900.

6. Stewart,G.S., Panier,S., Townsend,K., Al-Hakim,A.K., Kolas,N.K., Miller,E.S., Nakada,S., Ylanko,J., Olivarius,S., Mendez,M. *et al.* (2009) The RIDDLE syndrome protein mediates a ubiquitin-dependent signaling cascade at sites of DNA damage. *Cell*, **136**, 420–434.

7. Fradet-Turcotte,A., Canny,M.D., Escribano-Diaz,C., Orthwein,A., Leung,C.C., Huang,H., Landry,M.C., Kitevski-LeBlanc,J., Noordermeer,S.M., Sicheri,F. *et al.* (2013) 53BP1 is a reader of the DNA-damage-induced H2A Lys 15 ubiquitin mark. *Nature*, **499**, 50–54.

8. Gatti,M., Pinato,S., Maspero,E., Soffientini,P., Polo,S. and Penengo,L. (2012) A novel ubiquitin mark at the N-terminal tail of histone H2As targeted by RNF168 ubiquitin ligase. *Cell Cycle*, **11**, 2538–2544.

9. Mattiroli,F., Vissers,J.H., van Dijk,W.J., Ikpa,P., Citterio,E., Vermeulen,W., Marteijn,J.A. and Sixma,T.K. (2012) RNF168 ubiquitinates K13–15 on H2A/H2AX to drive DNA damage signaling. *Cell*, **150**, 1182–1195.

10. Bunting,S.F., Callen,E., Wong,N., Chen,H.T., Polato,F., Gunn,A., Bothmer,A., Feldhahn,N., Fernandez-Capetillo,O., Cao,L. *et al.* (2010) 53BP1 inhibits homologous recombination in Brca1-deficient cells by blocking resection of DNA breaks. *Cell*, **141**, 243–254.

11. Callen,E., Di Virgilio,M., Kruhlak,M.J., Nieto-Soler,M., Wong,N., Chen,H.T., Faryabi,R.B., Polato,F., Santos,M., Starnes,L.M. *et al.* (2013) 53BP1 mediates productive and mutagenic DNA repair through distinct phosphoprotein interactions. *Cell*, **153**, 1266–1280.

12. Chapman,J.R., Barral,P., Vannier,J.B., Borel,V., Steger,M., Tomas-Loba,A., Sartori,A.A., Adams,I.R., Batista,F.D. and Boulton,S.J. (2013) RIF1 is essential for 53BP1-dependent nonhomologous end joining and suppression of DNA double-strand break resection. *Mol. Cell*, **49**, 858–871.

13. Chapman,J.R., Sossick,A.J., Boulton,S.J. and Jackson,S.P. (2012) BRCA1-associated exclusion of 53BP1 from DNA damage sites underlies temporal control of DNA repair. *J. Cell Sci.*, **125**, 3529–3534.

14. Di Virgilio,M., Callen,E., Yamane,A., Zhang,W., Jankovic,M., Gitlin,A.D., Feldhahn,N., Resch,W., Oliveira,T.Y., Chait,B.T. *et al.* (2013) Rif1 prevents resection of DNA breaks and promotes immunoglobulin class switching. *Science*, **339**, 711–715.

15. Escribano-Diaz,C., Orthwein,A., Fradet-Turcotte,A., Xing,M., Young,J.T., Tkac,J., Cook,M.A., Rosebrock,A.P., Munro,M., Canny,M.D. *et al.* (2013) A cell cycle-dependent regulatory circuit composed of 53BP1-RIF1 and BRCA1-CtIP controls DNA repair pathway choice. *Mol. Cell*, **49**, 872–883.

16. Feng,L., Fong,K.W., Wang,J., Wang,W. and Chen,J. (2013) RIF1 counteracts BRCA1-mediated end resection during DNA repair. *J. Biol. Chem.*, **288**, 11135–11143.

17. Kakarougkas,A., Ismail,A., Katsuki,Y., Freire,R., Shibata,A. and Jeggo,P.A. (2013) Co-operation of BRCA1 and POH1 relieves the barriers posed by 53BP1 and RAP80 to resection. *Nucleic Acids Res.*, **41**, 10298–10311.

18. Zimmermann,M., Lottersberger,F., Buonomo,S.B., Sfeir,A. and de Lange,T. (2013) 53BP1 regulates DSB repair using Rif1 to control 5' end resection. *Science*, **339**, 700–704.

19. Farmer,H., McCabe,N., Lord,C.J., Tutt,A.N., Johnson,D.A., Richardson,T.B., Santarosa,M., Dillon,K.J., Hickson,I., Knights,C. *et al.* (2005) Targeting the DNA repair defect in BRCA mutant cells as a therapeutic strategy. *Nature*, **434**, 917–921.

20. Shen,S.X., Weaver,Z., Xu,X., Li,C., Weinstein,M., Chen,L., Guan,X.Y., Ried,T. and Deng,C.X. (1998) A targeted disruption of the murine Brca1 gene causes gamma-irradiation hypersensitivity and genetic instability. *Oncogene*, **17**, 3115–3124.

21. Honjo,T., Kinoshita,K. and Muramatsu,M. (2002) Molecular mechanism of class switch recombination: linkage with somatic hypermutation. *Annu. Rev. Immunol.*, **20**, 165–196.

22. Matthews,A.J., Zheng,S., DiMenna,L.J. and Chaudhuri,J. (2014) Regulation of immunoglobulin class-switch recombination: choreography of noncoding transcription, targeted DNA deamination, and long-range DNA repair. *Adv. Immunol.*, **122**, 1–57.

23. Petersen,S., Casellas,R., Reina-San-Martin,B., Chen,H.T., Difilippantonio,M.J., Wilson,P.C., Hanitsch,L., Celeste,A., Muramatsu,M., Pilch,D.R. *et al.* (2001) AID is required to initiate Nbs1/gamma-H2AX focus formation and mutations at sites of class switching. *Nature*, **414**, 660–665.

24. Daniel,J.A. and Nussenzweig,A. (2013) The AID-induced DNA damage response in chromatin. *Mol. Cell*, **50**, 309–321.

25. Rada,C., Williams,G.T., Nilsen,H., Barnes,D.E., Lindahl,T. and Neuberger,M.S. (2002) Immunoglobulin isotype switching is inhibited and somatic hypermutation perturbed in UNG-deficient mice. *Curr. Biol.*, **12**, 1748–1755.

26. Manis,J.P., Morales,J.C., Xia,Z., Kutok,J.L., Alt,F.W. and Carpenter,P.B. (2004) 53BP1 links DNA damage-response pathways to immunoglobulin heavy chain class-switch recombination. *Nat. Immunol.*, **5**, 481–487.

27. Ward,I.M., Reina-San-Martin,B., Olaru,A., Minn,K., Tamada,K., Lau,J.S., Cascalho,M., Chen,L., Nussenzweig,A., Livak,F. *et al.* (2004) 53BP1 is required for class switch recombination. *J. Cell Biol.*, **165**, 459–464.

28. Bothmer,A., Robbiani,D.F., Di Virgilio,M., Bunting,S.F., Klein,I.A., Feldhahn,N., Barlow,J., Chen,H.T., Bosque,D., Callen,E. *et al.* (2011) Regulation of DNA end joining, resection, and immunoglobulin class switch recombination by 53BP1. *Mol. Cell*, **42**, 319–329.

29. Bothmer,A., Robbiani,D.F., Feldhahn,N., Gazumyan,A., Nussenzweig,A. and Nussenzweig,M.C. (2010) 53BP1 regulates DNA resection and the choice between classical and alternative end joining during class switch recombination. *J. Exp. Med.*, **207**, 855–865.

30. Bothmer,A., Rommel,P.C., Gazumyan,A., Polato,F., Reczek,C.R., Muellenbeck,M.F., Schaetzlein,S., Edelmann,W., Chen,P.L., Brosh,R.M. Jr *et al.* (2013) Mechanism of DNA resection during intrachromosomal recombination and immunoglobulin class switching. *J. Exp. Med.*, **210**, 115–123.

31. Reina-San-Martin,B., Chen,J., Nussenzweig,A. and Nussenzweig,M.C. (2007) Enhanced intra-switch region recombination during immunoglobulin class switch recombination in 53BP1-/- B cells. *Eur. J. Immunol.*, **37**, 235–239.

32. Munoz,M.C., Laulier,C., Gunn,A., Cheng,A., Robbiani,D.F., Nussenzweig,A. and Stark,J.M. (2012) RING finger nuclear factor RNF168 is important for defects in homologous recombination caused by loss of the breast cancer susceptibility factor BRCA1. *J. Biol. Chem.*, **287**, 40618–40628.

33. Munoz,M.C., Yanez,D.A. and Stark,J.M. (2014) An RNF168 fragment defective for focal accumulation at DNA damage is proficient for inhibition of homologous recombination in BRCA1 deficient cells. *Nucleic Acids Res.*, **12**, 7720–7733.

34. Nakada,S., Yonamine,R.M. and Matsuo,K. (2012) RNF8 regulates assembly of RAD51 at DNA double-strand breaks in the absence of BRCA1 and 53BP1. *Cancer Res.*, **72**, 4974–4983.

35. Bohgaki,T., Bohgaki,M., Cardoso,R., Panier,S., Zeegers,D., Li,L., Stewart,G.S., Sanchez,O., Hande,M.P., Durocher,D. *et al.* (2011) Genomic instability, defective spermatogenesis, immunodeficiency, and cancer in a mouse model of the RIDDLE syndrome. *PLoS Genet.*, **7**, e1001381.

36. Ramachandran,S., Chahwan,R., Nepal,R.M., Frieder,D., Panier,S., Roa,S., Zaheen,A., Durocher,D., Scharff,M.D. and Martin,A. (2010) The RNF8/RNF168 ubiquitin ligase cascade facilitates class switch recombination. *Proc. Natl. Acad. Sci. U.S.A.*, **107**, 809–814.

37. Gudjonsson,T., Altmeyer,M., Savic,V., Toledo,L., Dinant,C., Grofte,M., Bartkova,J., Poulsen,M., Oka,Y., Bekker-Jensen,S. *et al.* (2012) TRIP12 and UBR5 suppress spreading of chromatin ubiquitylation at damaged chromosomes. *Cell*, **150**, 697–709.

38. Santos,M.A., Huen,M.S., Jankovic,M., Chen,H.T., Lopez-Contreras,A.J., Klein,I.A., Wong,N., Barbancho,J.L., Fernandez-Capetillo,O., Nussenzweig,M.C. *et al.* (2010) Class

switching and meiotic defects in mice lacking the E3 ubiquitin ligase RNF8. *J. Exp. Med.*, **207**, 973–981.

39. Cancer Genome Atlas Network. (2012) Comprehensive molecular portraits of human breast tumours. *Nature*, **490**, 61–70.
40. Cancer Genome Atlas Research Network. (2011) Integrated genomic analyses of ovarian carcinoma. *Nature*, **474**, 609–615.
41. Cerami,E., Gao,J., Dogrusoz,U., Gross,B.E., Sumer,S.O., Aksoy,B.A., Jacobsen,A., Byrne,C.J., Heuer,M.L., Larsson,E. *et al.* (2012) The cBio cancer genomics portal: an open platform for exploring multidimensional cancer genomics data. *Cancer Discov.*, **2**, 401–404.
42. Gao,J., Aksoy,B.A., Dogrusoz,U., Dresdner,G., Gross,B., Sumer,S.O., Sun,Y., Jacobsen,A., Sinha,R., Larsson,E. *et al.* (2013) Integrative analysis of complex cancer genomics and clinical profiles using the cBioPortal. *Sci. Signal.*, **6**, pl1.
43. Xie,A., Hartlerode,A., Stucki,M., Odate,S., Puget,N., Kwok,A., Nagaraju,G., Yan,C., Alt,F.W., Chen,J. *et al.* (2007) Distinct roles of chromatin-associated proteins MDC1 and 53BP1 in mammalian double-strand break repair. *Mol. Cell*, **28**, 1045–1057.
44. Sartori,A.A., Lukas,C., Coates,J., Mistrik,M., Fu,S., Bartek,J., Baer,R., Lukas,J. and Jackson,S.P. (2007) Human CtIP promotes DNA end resection. *Nature*, **450**, 509–514.
45. Cruz-Garcia,A., Lopez-Saavedra,A. and Huertas,P. (2014) BRCA1 accelerates CtIP-mediated DNA-end resection. *Cell Rep.*, **9**, 451–459.
46. Kousholt,A.N., Fugger,K., Hoffmann,S., Larsen,B.D., Menzel,T., Sartori,A.A. and Sorensen,C.S. (2012) CtIP-dependent DNA resection is required for DNA damage checkpoint maintenance but not initiation. *J. Cell Biol.*, **197**, 869–876.
47. Shiotani,B., Nguyen,H.D., Hakansson,P., Marechal,A., Tse,A., Tahara,H. and Zou,L. (2013) Two distinct modes of ATR activation orchestrated by Rad17 and Nbs1. *Cell Rep.*, **3**, 1651–1662.
48. Difilippantonio,S., Gapud,E., Wong,N., Huang,C.Y., Mahowald,G., Chen,H.T., Kruhlak,M.J., Callen,E., Livak,F., Nussenzweig,M.C. *et al.* (2008) 53BP1 facilitates long-range DNA end-joining during V(D)J recombination. *Nature*, **456**, 529–533.
49. Daley,J.M. and Sung,P. (2014) 53BP1, BRCA1, and the choice between recombination and end joining at DNA double-strand breaks. *Mol. Cell. Biol.*, **34**, 1380–1388.
50. Panier,S. and Boulton,S.J. (2014) Double-strand break repair: 53BP1 comes into focus. *Nat. Rev. Mol. Cell. Biol.*, **15**, 7–18.
51. Zimmermann,M. and de Lange,T. (2014) 53BP1: pro choice in DNA repair. *Trends Cell Biol.*, **24**, 108–117.
52. Cao,L., Xu,X., Bunting,S.F., Liu,J., Wang,R.H., Cao,L.L., Wu,J.J., Peng,T.N., Chen,J., Nussenzweig,A. *et al.* (2009) A selective requirement for 53BP1 in the biological response to genomic instability induced by Brca1 deficiency. *Mol. Cell*, **35**, 534–541.
53. Bouwman,P., Aly,A., Escandell,J.M., Pieterse,M., Bartkova,J., van der Gulden,H., Hiddingh,S., Thanasoula,M., Kulkarni,A., Yang,Q. *et al.* (2010) 53BP1 loss rescues BRCA1 deficiency and is associated with triple-negative and BRCA-mutated breast cancers. *Nat. Struct. Mol. Biol.*, **17**, 688–695.
54. Grotsky,D.A., Gonzalez-Suarez,I., Novell,A., Neumann,M.A., Yaddanapudi,S.C., Croke,M., Martinez-Alonso,M., Redwood,A.B., Ortega-Martinez,S., Feng,Z. *et al.* (2013) BRCA1 loss activates cathepsin L-mediated degradation of 53BP1 in breast cancer cells. *J. Cell Biol.*, **200**, 187–202.
55. Jaspers,J.E., Kersbergen,A., Boon,U., Sol,W., van Deemter,L., Zander,S.A., Drost,R., Wientjens,E., Ji,J., Aly,A. *et al.* (2013) Loss of 53BP1 causes PARP inhibitor resistance in Brca1-mutated mouse mammary tumors. *Cancer Discov.*, **3**, 68–81.
56. Jacot,W., Thezenas,S., Senal,R., Viglianti,C., Laberenne,A.C., Lopez-Crapez,E., Bibeau,F., Bleuse,J.P., Romieu,G. and Lamy,P.J. (2013) BRCA1 promoter hypermethylation, 53BP1 protein expression and PARP-1 activity as biomarkers of DNA repair deficit in breast cancer. *BMC Cancer*, **13**, 523.
57. Pennington,K.P., Wickramanayake,A., Norquist,B.M., Pennil,C.C., Garcia,R.L., Agnew,K.J., Taniguchi,T., Welcsh,P. and Swisher,E.M. (2013) 53BP1 expression in sporadic and inherited ovarian carcinoma: Relationship to genetic status and clinical outcomes. *Gynecol. Oncol.*, **128**, 493–499.
58. Robbiani,D.F., Bunting,S., Feldhahn,N., Bothmer,A., Camps,J., Deroubaix,S., McBride,K.M., Klein,I.A., Stone,G., Eisenreich,T.R. *et al.* (2009) AID produces DNA double-strand breaks in non-Ig genes and mature B cell lymphomas with reciprocal chromosome translocations. *Mol. Cell*, **36**, 631–641.